5. DYNAMICS OF SIMPLIFIED TWO-AXLE BOGIES

5.1. INTRODUCTION

This chapter reports the modelling of simplified two-axle bogies using the Rail Bogie Dynamic (RBD) Program. As most of the wagons and passenger cars use this type of bogie, the examination of its dynamics has become a subject of interest to railway engineers and researchers for many years. Thus this type of bogie was considered in evaluating the capability of the RBD program.

First, the bogie dynamics under constant speed are reported and the results are validated against VAMPIRE. Second, the RBD program has been used to simulate the effect of the longitudinal braking and traction forces to the speed profile and the associated lateral, vertical and pitch dynamics of the bogie. The results of the simulation under the variable speed profile have also been validated using VAMPIRE; for this purpose the output speed profile calculated by the RBD program has been used as input for the VAMPIRE simulation. The capability of the RBD program to simulate severe bogie dynamics with the associated wheel skid is also demonstrated in this chapter. To the best knowledge of the author, no wagon dynamics commercial programs possess the capability of skid analysis.

5.2. DESCRIPTION OF MODELLED SYSTEM

The system of a simplified two-axle bogie containing one bogie frame and two wheelsets is shown in Fig.5.1. The distance between axles was 1.675 mm (distance between axles of most of QR three-piece bogie)

a.) Top View

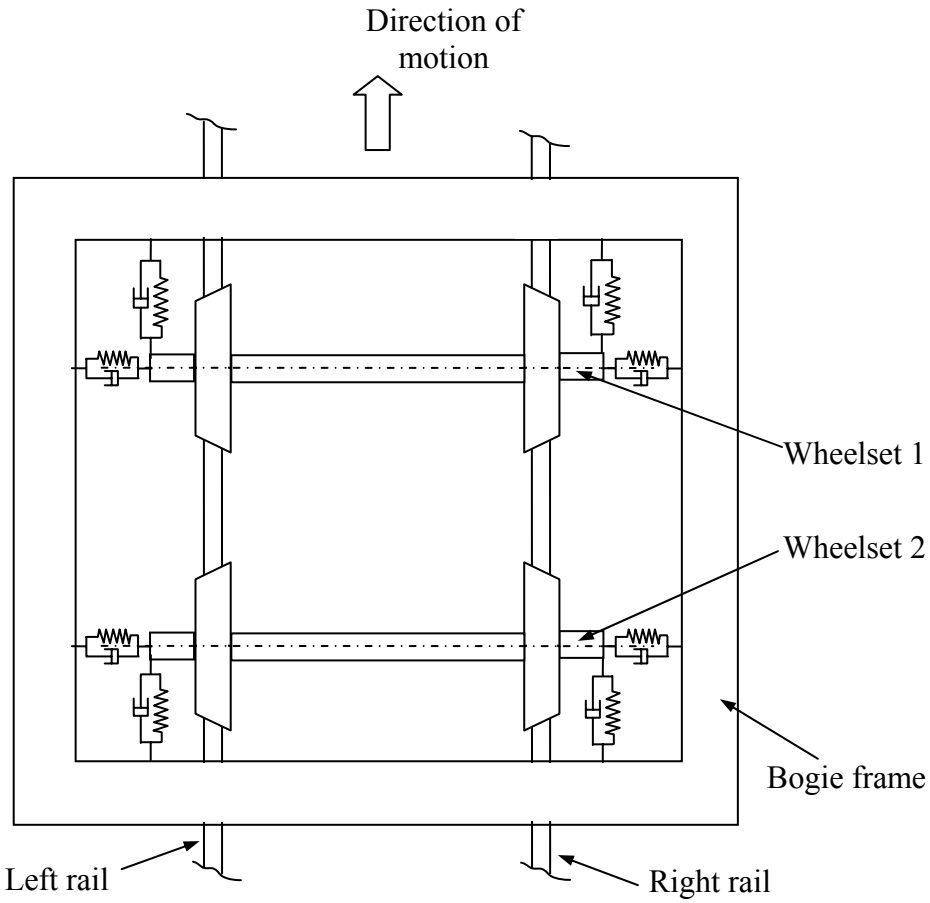

b.) Front View

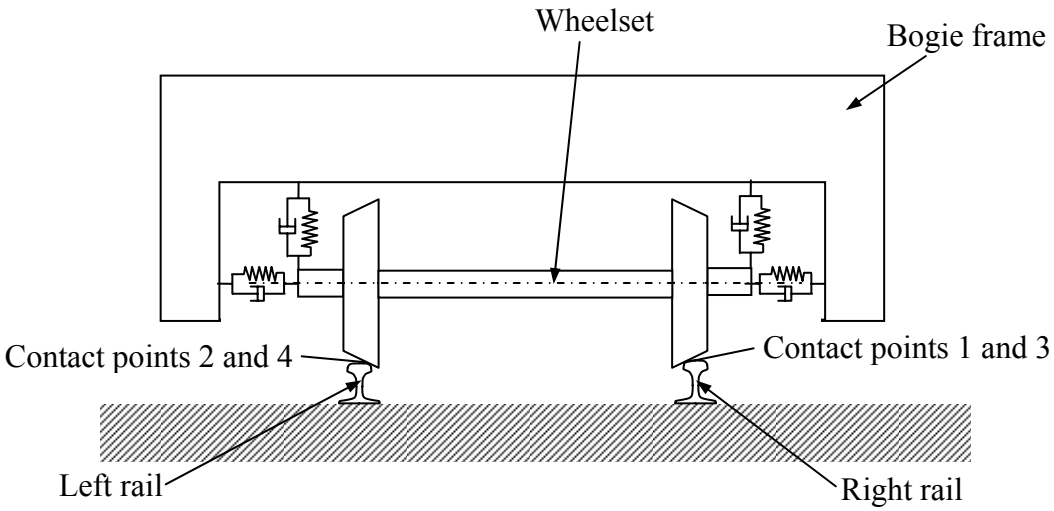

Figure 5.1. Simplified two-axle bogie

Each wheelset is connected to the bogie frame by a set of linear springs and dampers. The total number of bodies involved was five; the bogie frame, the leading wheelset (wheelset 1), the trailing wheelset (wheelset 2), the left rail and the right rail. All the bodies were assumed as rigid with the body reference frames attached to their respective centres of mass. The coordinate system is described using the same convention as defined in Section 2.1. Adopting the formulation in Chapter 3, the motion of each body's local coordinate system with respect to the global system is described in the multibody formulation using three translational coordinates and four Euler parameters. The vector of generalised coordinates of the modelled system that contains five bodies can now be written as:

$$\mathbf{q} = \begin{bmatrix} \mathbf{q}^{rr} & \mathbf{q}^{rl} & \mathbf{q}^{ws1} & \mathbf{q}^{ws2} & \mathbf{q}^{bf} \end{bmatrix}^{\mathrm{T}} \tag{5.1}$$

where $\mathbf{q}^{rr}, \mathbf{q}^{rl}, \mathbf{q}^{ws1}, \mathbf{q}^{ws2}, \mathbf{q}^{bf}$ are vectors of generalised coordinates of the right rail, the left rail, the leading wheelset (ws1), the trailing wheelset (ws2) and the bogie frame respectively. Because each body has three translational coordinates and four Euler parameters, the total vector coordinates in Eq.5.1 will have 35 components.

There are four contact points involved in the system. Thus, the vector of non-generalised surface parameters is written as

$$\mathbf{s} = \begin{bmatrix} \mathbf{s}_1^{rr} & \mathbf{s}_2^{rl} & \mathbf{s}_3^{rr} & \mathbf{s}_4^{rl} & \mathbf{s}_1^{ws1} & \mathbf{s}_2^{ws1} & \mathbf{s}_3^{ws2} & \mathbf{s}_4^{ws2} \end{bmatrix}^{\mathrm{T}} \tag{5.2}$$

where each superscript represents a body as described in Eq.(5.1) and the subscript represents the number of contact points:

- contact point 1 is located at the *right* wheel-rail patch of the *leading* wheelset
- contact point 2 is located at the *left* wheel-rail patch of the *leading* wheelset

- contact point 3 is located at the *right* wheel-rail patch of the *trailing* wheelset
- contact point 4 is located at the *left* wheel-rail patch of the *trailing* wheelset

Because each contact surface is represented by two surface parameters, vectors of non-generalised surface parameters in Eq.(5.2) will have sixteen components. Thus, in total, the vector of generalised and non-generalised coordinates will have 51 components.

Through the introduction of five Euler parameter constraints (one for each body), 20 contact constraints, and twelve ground constraints, there have been a total of 37 constraint equations associated with fourteen (51-37=14) unrestrained degrees of freedom. As there are 37 constraint equations, 35 generalised coordinates, and 16 non-generalised surface parameters, the size of sub-Jacobian matrix $\mathbf{C}_\mathbf{q}$ is 37×35 and the size of sub-Jacobian matrix $\mathbf{C}_\mathbf{s}$ is 37×16. Hence, for the system of the simplified two-axle bogie, the total dimension of the augmented matrix of the mass matrices and sub-Jacobian matrices in Eq.(3.75) was 88×88. For the constant speed simulation a velocity constraint in the longitudinal direction was added, which increased the dimension of the augmented matrix to 89×89 and reduced the unrestrained degrees of freedom to thirteen.

The characteristics of the springs and dampers of the bogie shown in Fig.5.1 are presented in Table 5.1. The inertia properties of the wheelsets and the lumped spring mass used in the simulation are given in Table.5.2. The inertia properties of the sprung mass were chosen so that the axle load represents the heavy haul wagon operation (approximately 300 kN). The spring stiffness and damping coefficient of the suspension was optimised so that the bogie remained stable (no wheelset hunting) at least up to 25

m/s (90 km/h). The wheel and the rail profiles used were the same as those presented in Section 4.3 of the previous chapter.

Table 5.1. Spring and damper characteristics

	Spring Stiffness , K (N/m)	Damping Coefficient, C (N.s/m)
Longitudinal	9.5×10^6	8×10^4
Lateral	6.0×10^6	4×10^4
Vertical	3.5×10^6	2.5×10^4

Table 5.2. Inertia properties of the wheelsets and the sprung mass

	Wheelset	Sprung Mass
Mass (kg)	1200	60,000
Mass moment of inertia I_{xx} ($\mathrm{kg \cdot m^2}$)	720	80,000
Mass moment of inertia I_{yy} ($\mathrm{kg \cdot m^2}$)	112	60,000
Mass moment of inertia I_{zz} ($\mathrm{kg \cdot m^2}$)	720	20,000

5.3. SIMULATION AT CONSTANT SPEED

5.3.1. Response to Lateral Track Irregularities

Response of the model to lateral disturbance has been studied. Instead of simply using the initial value of lateral displacement, a sinusoidal track irregularity as shown in Fig 5.2 was input to initiate the lateral oscillation.

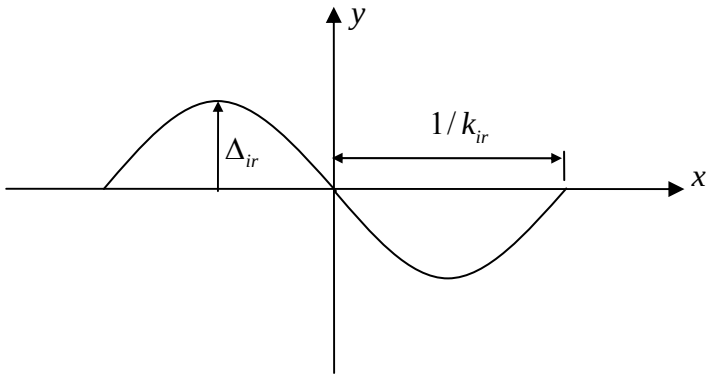

Figure 5.2. Parameters representing sinusoidal track irregularity

The analytical representation of the sinusoidal irregularity is expressed as shown in Eq. (5.3).

$$y(x) = \Delta_{ir} \sin \pi k_{ir} x \qquad (5.3)$$

where Δ_{ir} is the amplitude and k_{ir} is a parameter that defines the sine wavelength. For the lateral irregularity, a value in the range of $\Delta_{ir} = (0.0203 \sim 0.0305)\, m$ and $k_{ir} = (0.0426 \sim 0.0656)\ m^{-1}$ suggested by Garg and Dukkipati (1984) has been used in the simulation. Specific values adopted were $\Delta_{ir} = 0.025\ m$ and $k_{ir} = 0.045\ m^{-1}$, which corresponded to an amplitude of 0.025 m and wavelength of 44.44 m. The irregularity was assumed to occur at the fifth metre of travel as plotted in Fig 5.3. Some important results of the constant speed simulation at two selected speeds of 15 m/s (54 km/h) and 25 m/s (90 km/h) are presented in this section.

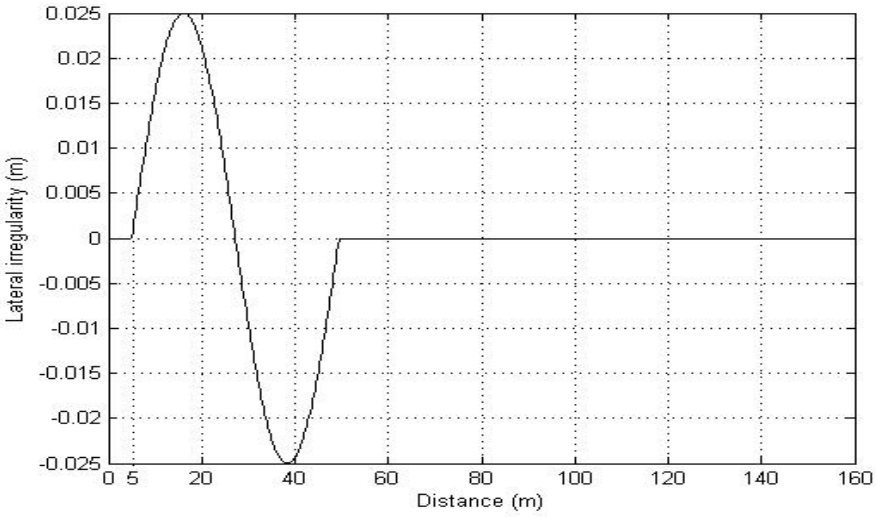

Figure 5.3. Input Lateral Track Irregularity

Response at 15 m/s (54 km/h)

Fig 5.4 shows the lateral displacement of the trailing and the leading wheelsets, relative to the centre of the track, against travel distance at 15 m/s (54 km/h) obtained by the RBD program. As expected, when running on the track containing lateral irregularity (from 5 m to 50 m travel distance) the wheelsets were subjected to a lateral displacement of 9.5 mm (exhibited by the leading wheelset at the travelling distance of 17 m). After passing the irregularity section the amplitude of the lateral oscillations decreased very quickly suggesting that at this speed the bogie was stable with very high level of damping. Fig.5.4 also reveals that the oscillation of the trailing wheelset was lagging in phase and had relatively lower amplitude. The marginal phase difference in time series between the leading and the trailing wheelsets corresponds to the speed of travel and the distance between the axles.

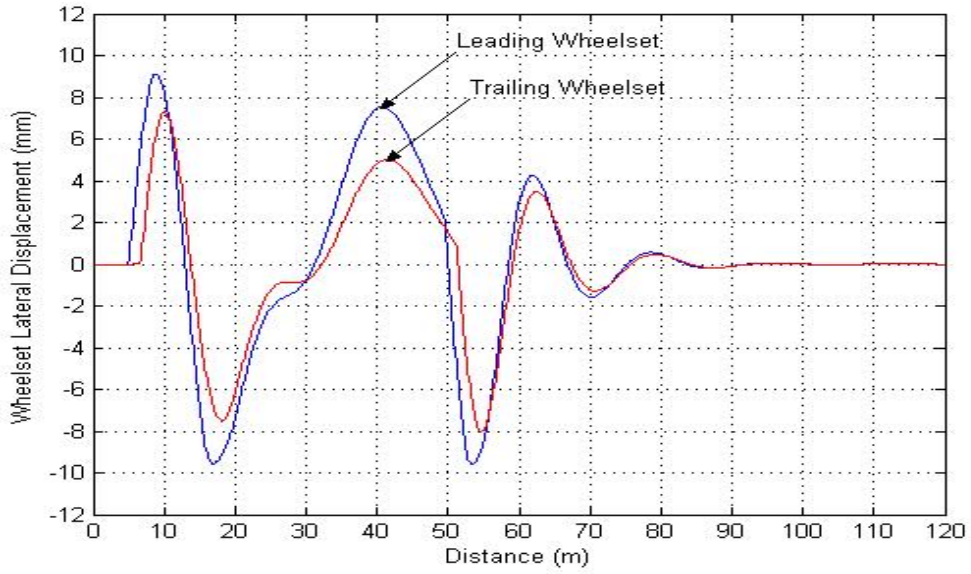

Figure 5.4. Wheelset lateral displacement - RBD program at V = 15 m/s

Figure 5.5. Wheelset lateral displacement - VAMPIRE at V = 15m/s

For comparison, the same system was also modelled using VAMPIRE software. The lateral displacement of the wheelsets calculated by VAMPIRE for the speed of 15 m/s

(54 km/h) are shown in Fig.5.5. This figure shows, in general, the same trend and magnitude as that provided by the RBD program presented in Fig 5.4. The maximum lateral displacement of the bogie due to the passage across the track section containing the sinusoidal irregularity was 10 mm, (0.5 mm larger than that calculated by the RBD program) occurring at the travel distance of 17 m (same as that predicted by the RBD program).

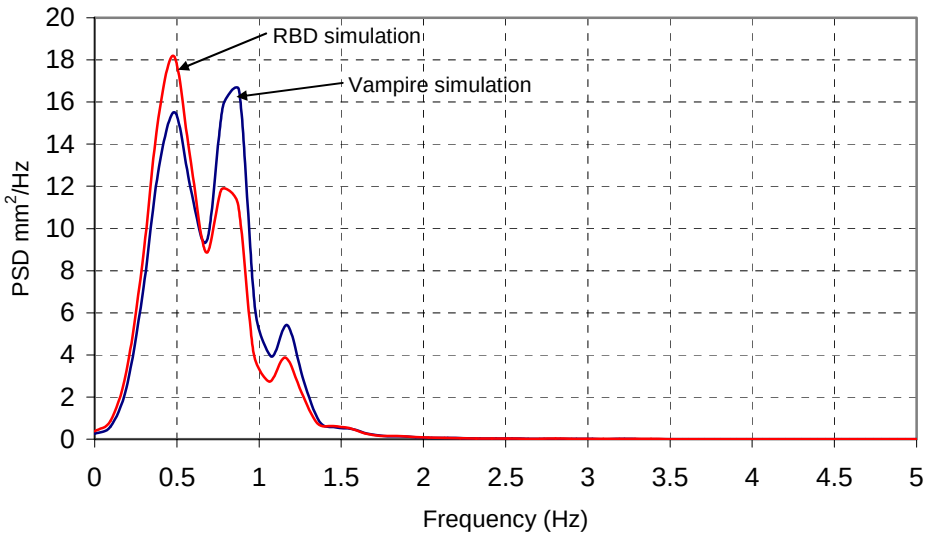

Figure 5.6. Frequency spectrum of the leading wheelset lateral oscillation at 15 m/s

Fig.5.6 shows the frequency spectrum of the oscillation of the leading wheelset calculated by the RBD program and VAMPIRE at a speed of 15 m/s. Both spectrums identify two high peaks. For the first peak, the RBD program obtained a frequency of 0.488 Hz and VAMPIRE obtained 0.483 Hz (1.04 % error); while for the second peak the RBD program calculated 0.774 Hz and VAMPIRE calculated 0.879 Hz (11.95 % error). The differences are considered insignificant. The peak at the lower frequency was related to the forced excitation due to the lateral irregularity, while the peak at the

higher frequency was related to the kinematic oscillation of the wheelsets due to their conicity.

The phase difference between the leading and the trailing wheelsets induces bogie frame yaw. The yaw of the bogie frame calculated by the RBD program (red line) and VAMPIRE (blue line) are presented in Fig.5.7. It can be seen that both of these results agree very well.

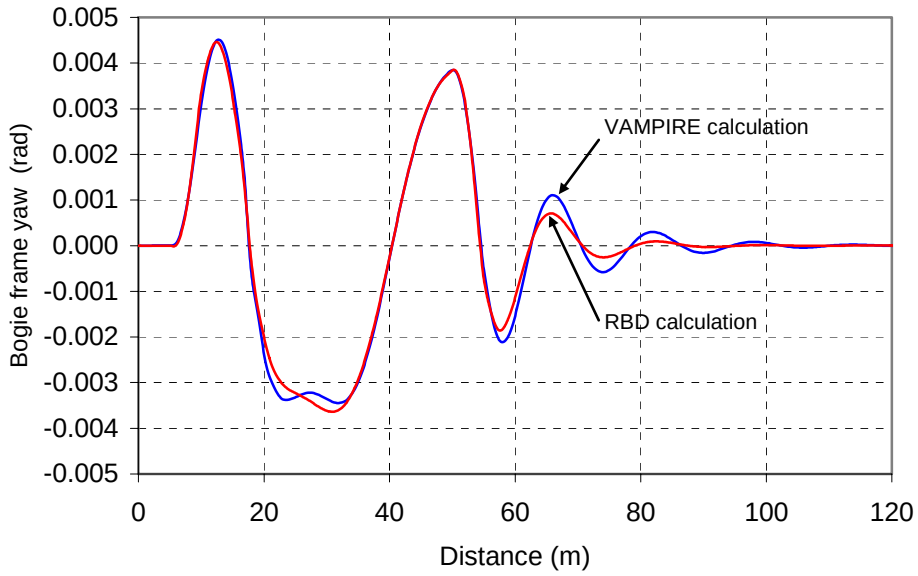

Figure 5.7. Bogie frame yaw at 15 m/s

Response at 25 m/s (72 km/h)

Fig 5.8 shows the lateral displacement of the trailing and the leading wheelsets obtained by the RBD program at a constant speed of 25 m/s while Fig 5.9 shows the same information calculated by VAMPIRE. Comparing both figures, it can be seen that in general the trend and magnitude of the wheelset lateral displacement calculated by the RBD program agree very well with that of the VAMPIRE simulation.

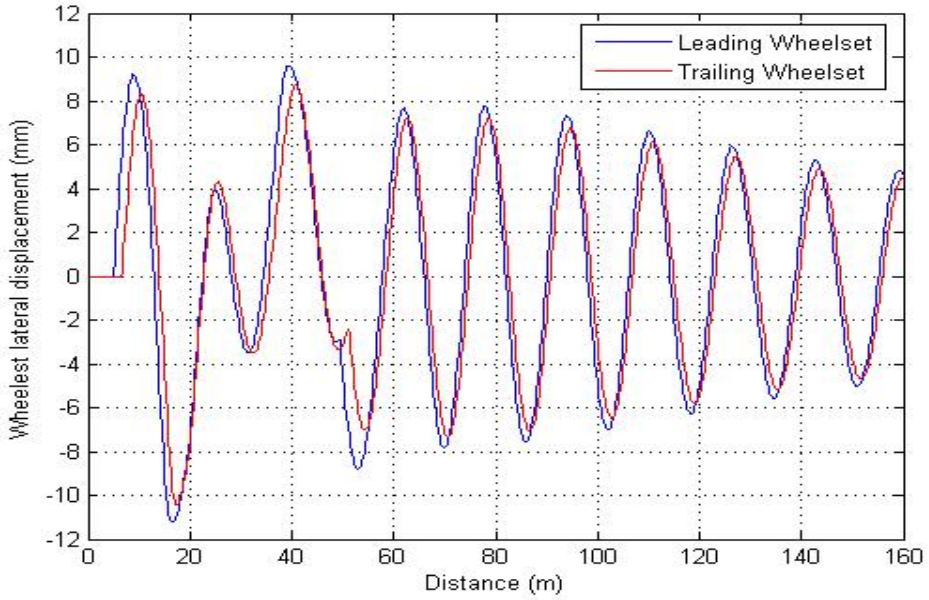

Figure 5.8. Wheelset lateral displacement calculation by RBD program at 25 m/s

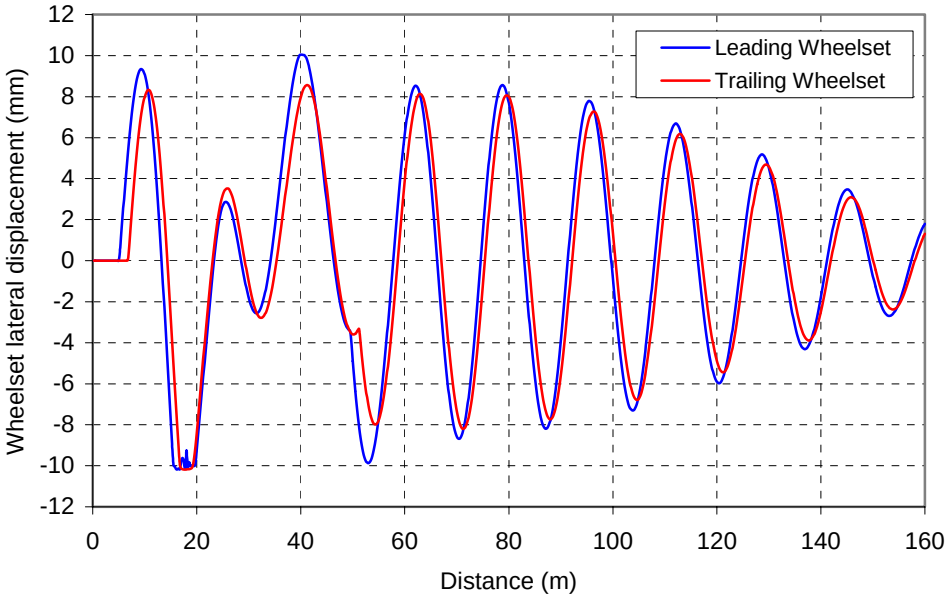

Figure 5.9. Wheelset lateral displacement calculation by VAMPIRE at 25 m/s

Fig.5.10 presents the frequency spectrum of the lateral oscillation of the leading wheelset at 25 m/s. Both the frequency spectrum of the lateral oscillation calculated by VAMPIRE and the RBD program exhibit similar trends where only one dominant peak

appears on the spectrum. This peak is related to the frequency of the kinematics oscillation due to the conicity of the wheelset. The RBD program predicted 89.01 mm^2/Hz peak at the frequency of 1.45 Hz while VAMPIRE predicted 106.44 mm^2/Hz peak at the frequency of 1.46 Hz. The difference in peak values calculated by VAMPIRE and the RBD program is insignificant.

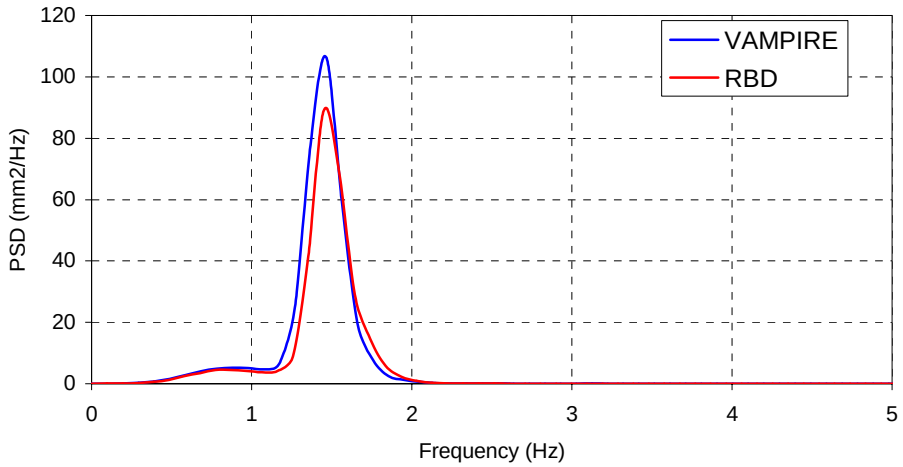

Figure 5.10. Frequency spectrum of the leading wheelset lateral oscillation at 25 m/s

The yaw of the bogie frame obtained from both simulations at 25 m/s are shown in Fig.5.11. As expected the yaw oscillation of the bogie frame follows the trend of the wheelset lateral oscillation, because the bogie frame yaw oscillation was initiated by the phase difference between the leading and the trailing wheelset lateral oscillations.

Simulations at the constant speeds of 15 m/s and 25 m/s reveal that the RBD program results are as good as, if not better than that of the VAMPIRE. Some inevitable differences have resulted due to the difference in the adopted methods of calculation of the contact parameters and creep forces as well as the method of numerical integration used. As has been explained previously, the creep forces were calculated using the

Polach formulation and the British Table Book derived from the Kalker Non-Linear formulation respectively by the RBD program and VAMPIRE.

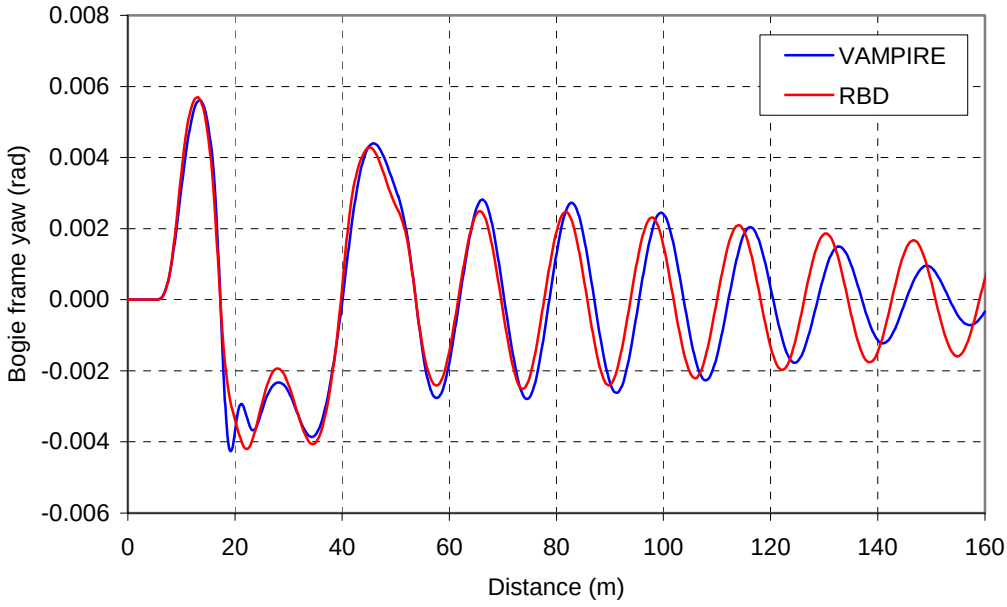

Figure 5.11. Bogie frame yaw 25 m/s

5.3.2. Response to Track Vertical Irregularity

With a view to examining the capability of the RBD program to predict dynamic response in the vertical direction we have considered vertical irregularity in the track profile as an input. A vertical disturbance in the form of a sinusoidal vertical irregularity was input. The analytical representation of the sinusoidal irregularity as expressed in Eq.(5.3) was used with the vertical irregularity parameters $\Delta_{ir} = (0.0254 \sim 0.0381)\ m$ and $k_{ir} = (0.0656 \sim 0.0820)\ m^{-1}$ (Garg and Dukkipati (1984)). For the simulation reported in this section the values of $\Delta_{ir} = 0.03\ m$ and $k_{ir} = 0.07\ m^{-1}$ were used. With the chosen parameter $k_{ir} = 0.07$, the corresponding wavelength of the irregularity was 28.57 m. The vertical irregularity was assumed to be

located at the fifth metre of travel as shown in Fig 5.12. Simulations were carried out at two constant speeds of 15 m/s (54 km/h) and 25 m/s (90 km/h).

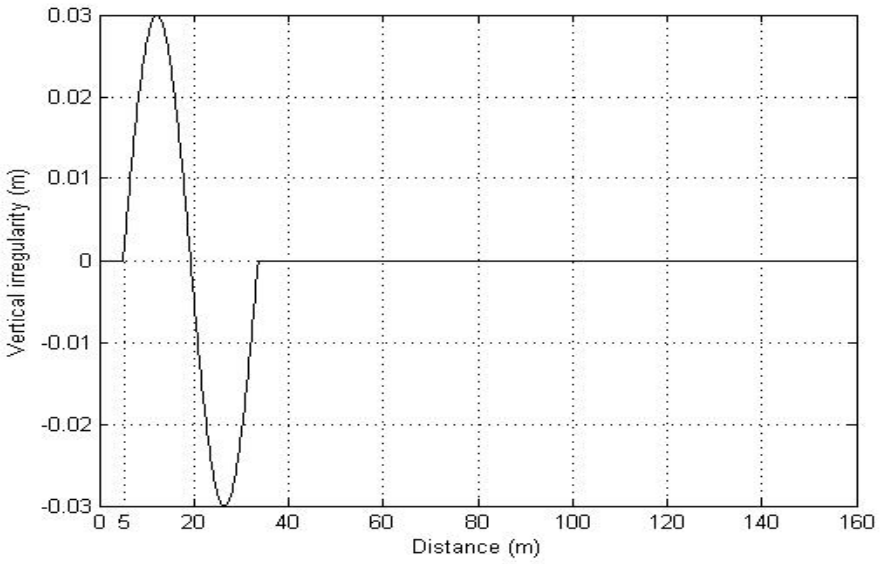

Figure 5.12. Input Track Vertical Irregularity

The dynamic response of the bogie frame in the vertical direction calculated by the RBD program at 15 m/s and 25 m/s due to the input of the track vertical irregularity is exhibited in Fig.5.13, while the corresponding response calculated using VAMPIRE is shown in Fig.5.14. It can be seen that the results calculated by the RBD program and VAMPIRE agree very well both at the low speed of 15 m/s and the high speed of 25 m/s. The amplitude and wavelength obtained from the RBD program were found to have almost exactly the same value as that obtained from VAMPIRE. The associated frequency spectrums of the bogie frame vertical oscillation calculated by the RBD program and VAMPIRE are shown in Fig.5.15 (a) and (b) respectively.

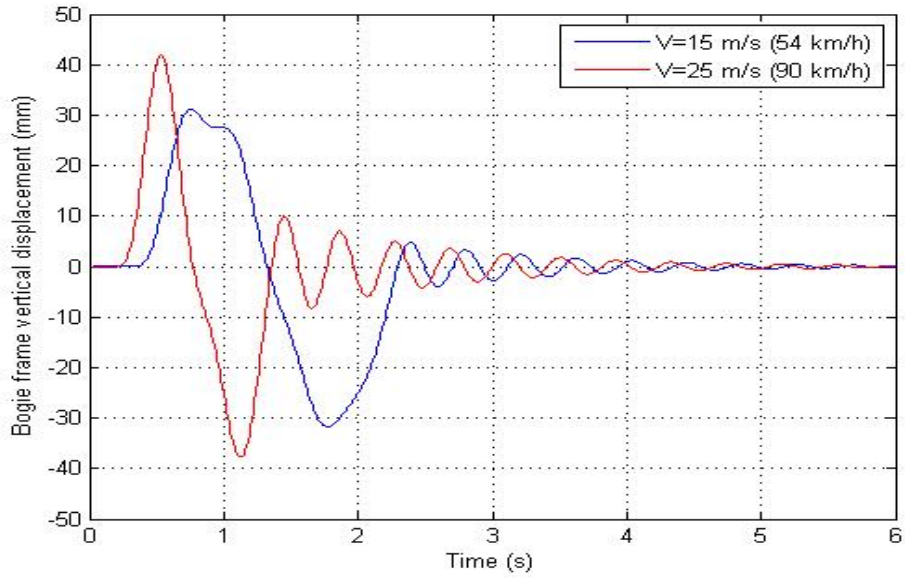

Figure 5.13. Bogie frame vertical displacement calculated by RBD program

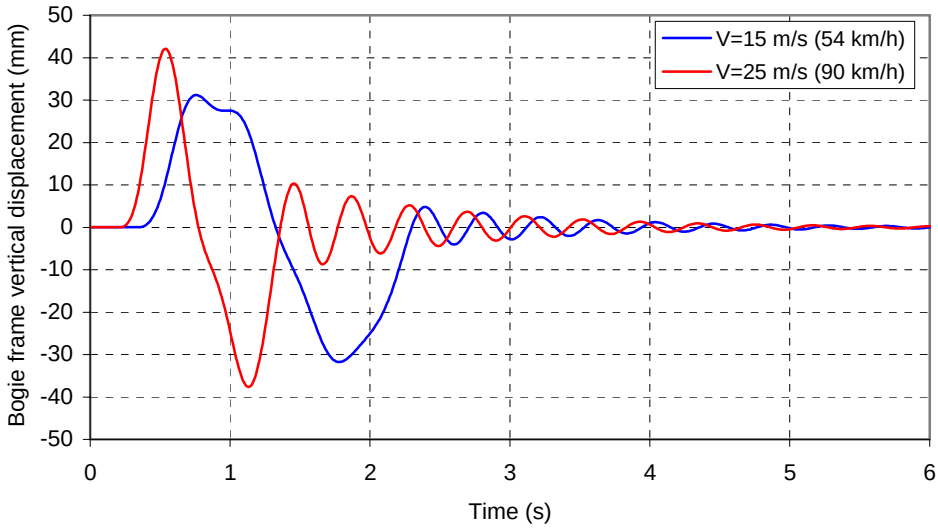

Figure 5.14. Bogie frame vertical displacement calculated by VAMPIRE

Two peaks are found in the frequency spectrum shown in Fig.5.15 (a) and (b). The peak at the low frequency is related to the forced excitation due to the track irregularity. The frequency of this peak normally changes with the change in speed. At the speed of 15 m/s the first peak has been found to occur at 0.48 Hz and 0.49 Hz respectively as per

predictions of the RBD program and VAMPIRE. At the speed of 25 m/s the first peak frequency has been determined as 0.77 Hz and 0.78 Hz respectively by RBD program and VAMPIRE. The second peak at the higher frequency is related to the natural frequency (2.31 Hz as calculated by the RBD program and 2.34 Hz as calculated by VAMPIRE) of the system in the vertical direction. The frequency of this second peak, therefore, has not changed with the changes of the speed of the bogie.

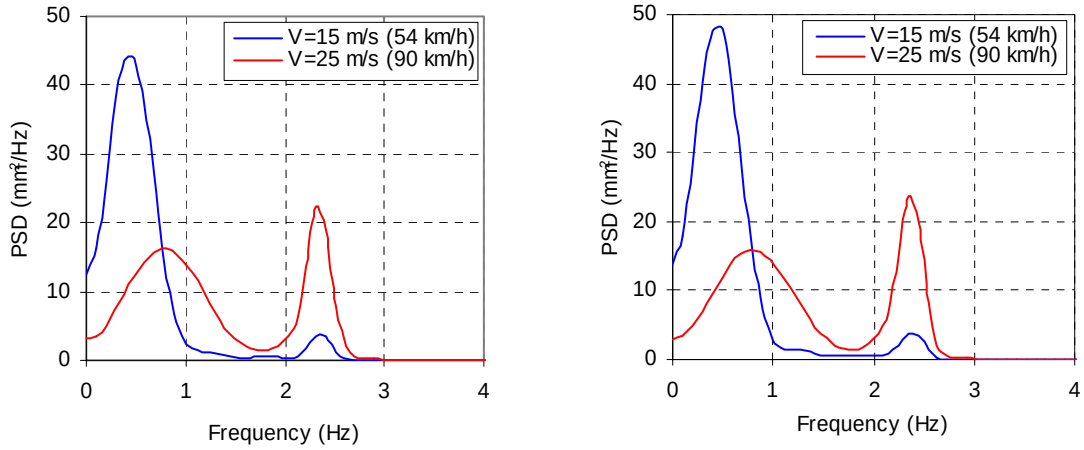

(a) RBD Program (b) VAMPIRE

Figure 5.15. Frequency spectrum of bogie frame vertical oscillation

Fig.5.16 presents the axle load time series due to the same sine wave vertical irregularity calculated by the RBD program at the speed of 15 m/s (Fig.5.16.a) and 25 m/s (Fig.5.16.b). It also agrees very well with the similar information calculated by VAMPIRE shown in Fig 5.17 (a) and (b). The different phase of the axle load oscillation between the leading and the trailing wheelset shows that the given vertical irregularity also generated bogie pitch because both wheelsets did not contact the track irregularity at the same time; the delay was due to the distance between axles and the running speed.

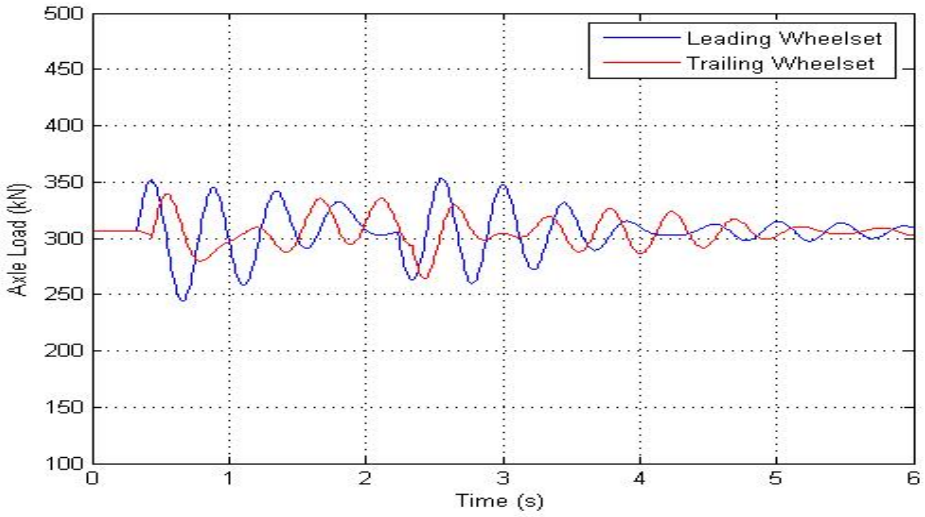

(a.) V = 15 m/s (54 km/h)

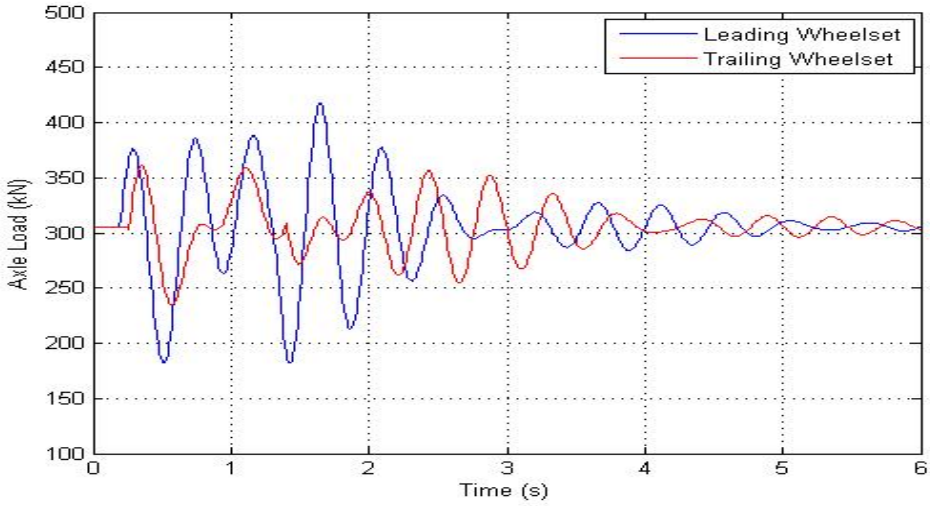

(b.) V=25 m/s (90 km/h)

Figure 5.16. Axle load due to vertical irregularity calculated by RBD program

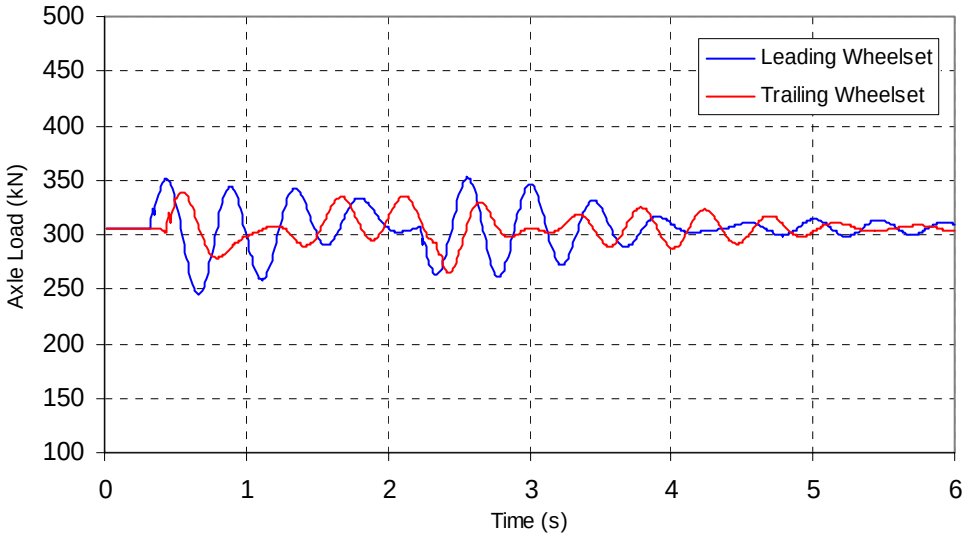

(a.) V=15 m/s (54 km/h)

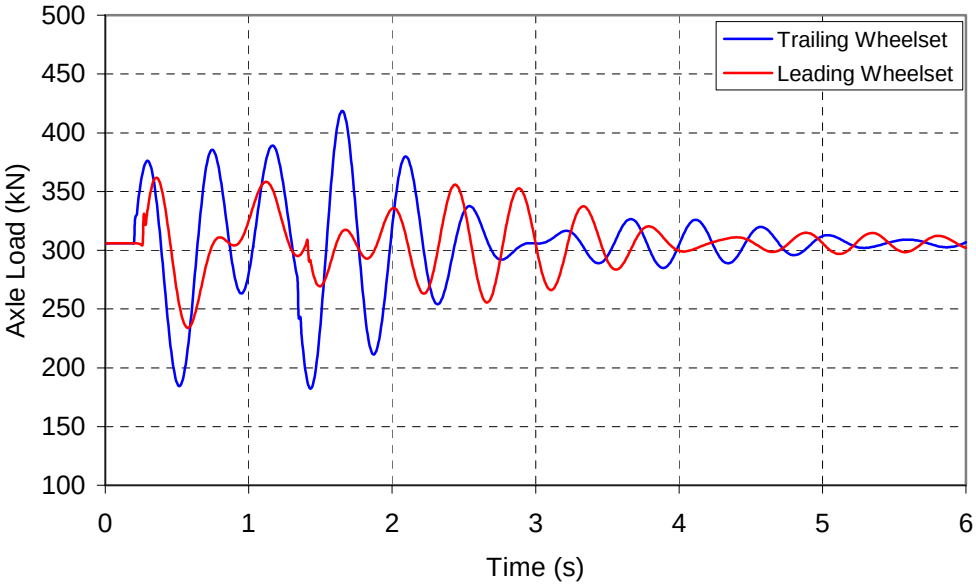

(b.)V=25 m/s (90 km/h)

Figure 5.17. Axle load due to vertical irregularity calculated by VAMPIRE

5.3.3. Response to Track Cross Level Irregularity

Response of the system to cross-level irregularity was also studied. Cross-level irregularity is defined as the height difference between the right and the left rail (see Section 2.4). It is assumed to be positive if the left rail is higher than the right rail when the observer is facing the running direction of the bogie. A typical form of the cross level irregularity, which is called a "plateau" is shown in Fig.5.18.

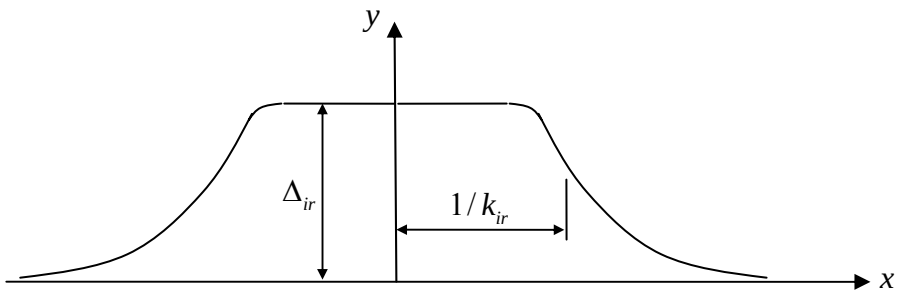

Figure 5.18. Cross level plateau irregularity and its parameters

The analytical representation of the plateau can be expressed as:

$$y(x) = \left(\frac{{\Delta_{ir}}^2}{1 + (k_{ir} x)^8} \right)^{1/2} \qquad (5.4)$$

where x is the longitudinal travel and y is the height difference between the right and the left rails. For the simulation reported in this section the values of $\Delta_{ir} = 0.02\ m$ and $k_{ir} = 0.07\ m^{-1}$ have been used based on the range of values given by Garg and Dukkipati (1984), which gives the plateau irregularity as shown in Fig.5.19.

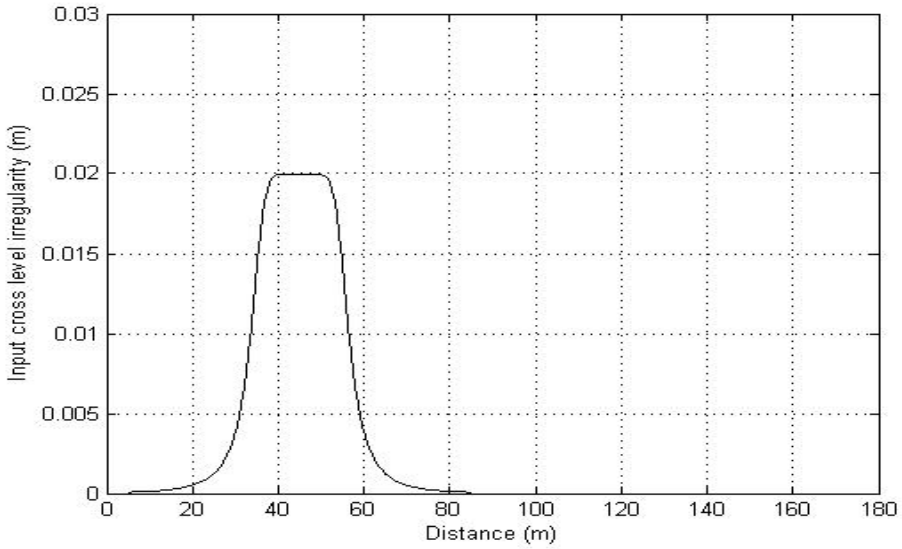

Figure 5.19. Input cross level irregularity

The input of cross-level irregularity caused the rolling motion of the bogie as revealed in Fig.5.20 calculated by the RBD program at the speed of 15 m/s (54 km/h) and 25 m/s (90 km/h). In general, this result agrees very well with that of VAMPIRE shown in Fig.5.21.

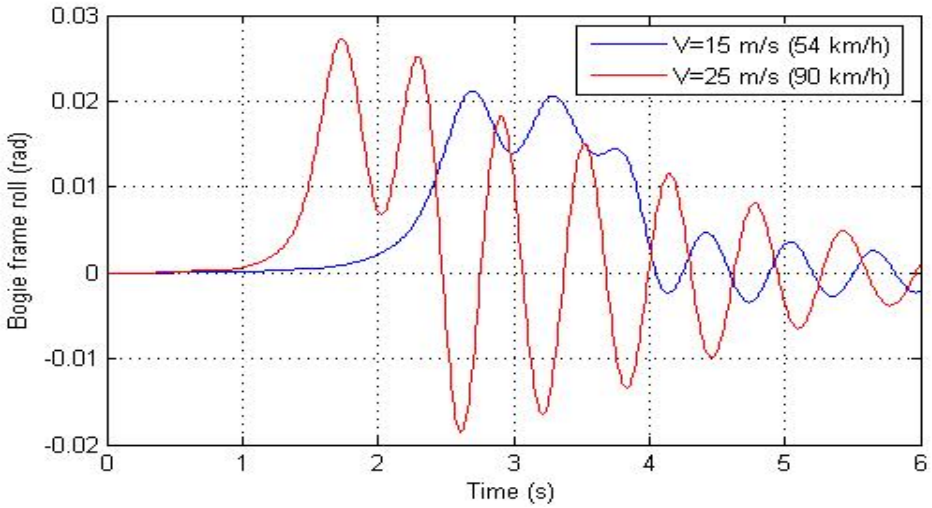

Figure 5.20. Bogie frame roll calculated by RBD program

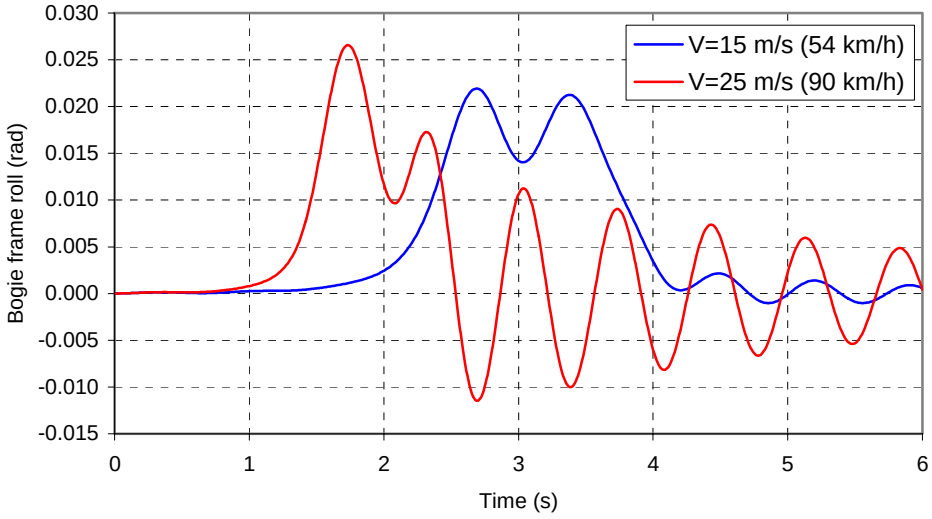

Figure 5.21. Bogie frame roll calculated by VAMPIRE

The maximum roll occurred at the track section containing the irregularity. At 15 m/s and 25 m/s, the RBD program calculated maximum rolling of 0.021 radian and 0.028 radian respectively; and VAMPIRE gave 0.022 radian and 0.027 radian respectively.

The calculated wheel load time series from the RBD program at the right and the left wheel of the leading wheelset due to this cross-level irregularity is exhibited in Figure 5.22 and the result calculated by VAMPIRE is presented in Fig 5.23. At the speed of 15 m/s the RBD program recorded 188 kN maximum value while VAMPIRE obtained 169 kN (approximately 11 % error margin). At the speed of 25 m/s the RBD program calculated 243 kN while VAMPIRE gave 224 kN (approximately 8 % error margin). The opposite phase of the wheel load between the left and the right rail shows that the bogie was subjected to rolling motion.

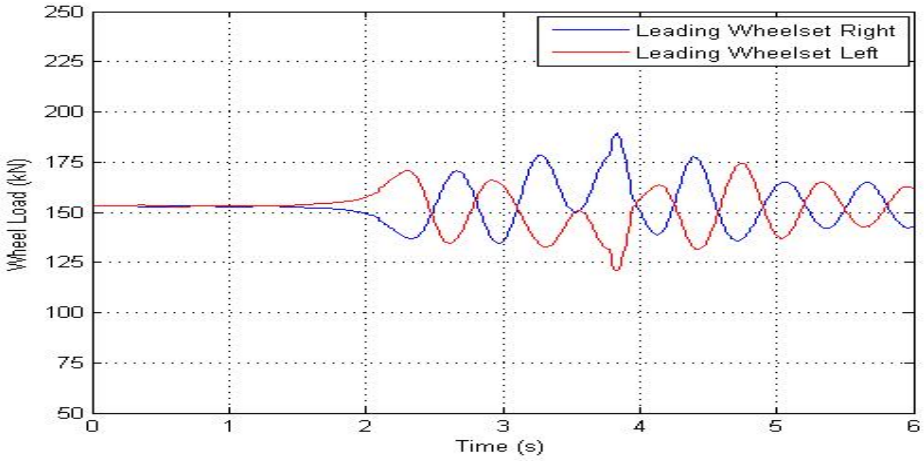

(a.) V=15 m/s (54 km/h)

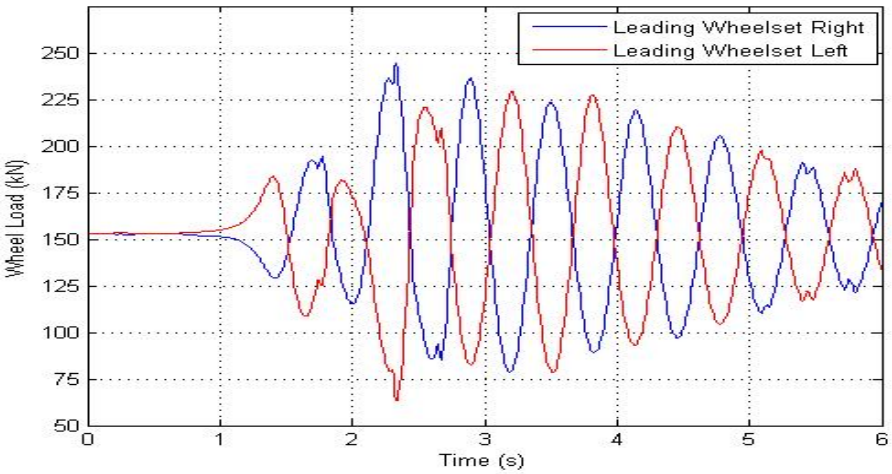

(b.) V=25 km/h (90 km/h)

Figure 5.22. Wheel load due to cross level irregularity calculated by RBD program

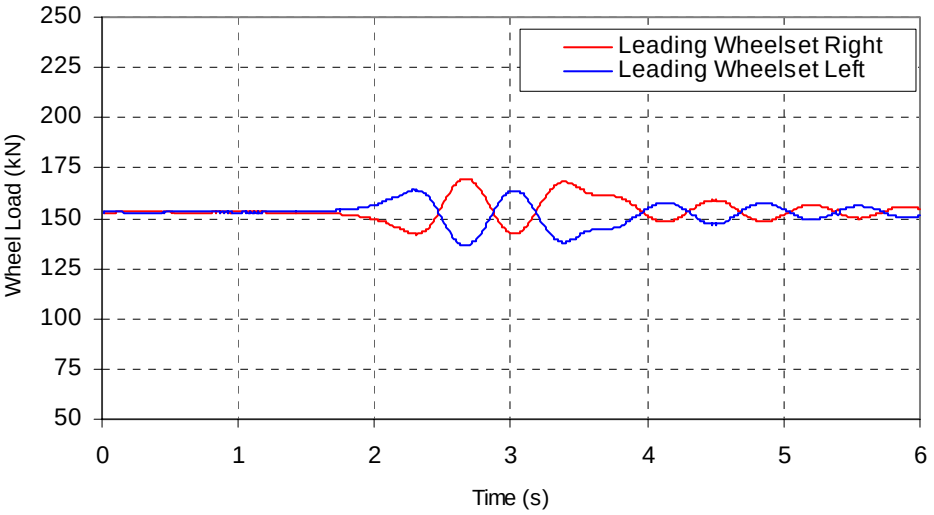

(a.) V=15 m/s (54 km/h)

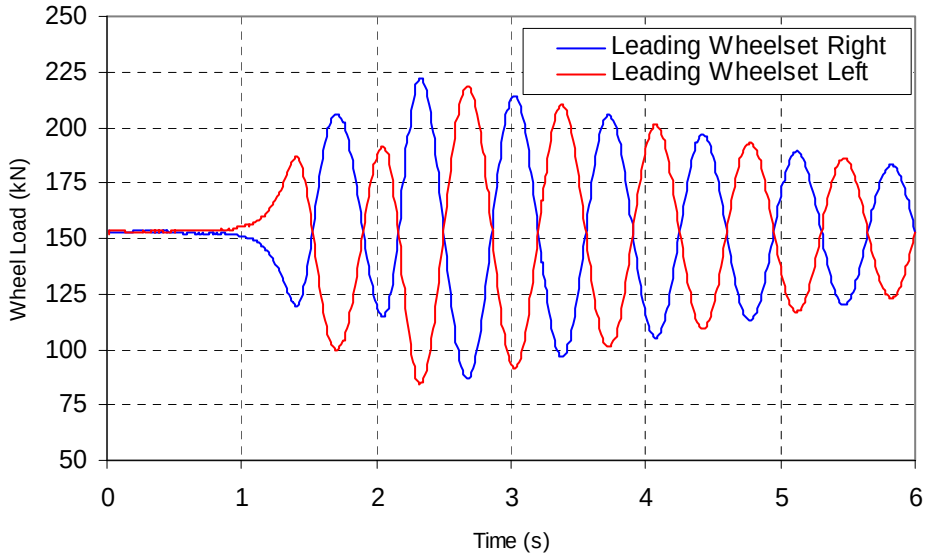

(b.) V=25 m/s (90 km/h)

Figure 5.23. Wheel load due to cross level irregularity calculated by VAMPIRE

5. 4. APPLICATION OF LONGITUDINAL FORCE

5.4.1. Speed Profile

The simulation reported in this section is intended to examine the capability of the RBD program to calculate the speed profile due to the application of the longitudinal force. For this purpose, a sequence of traction and braking torques was applied to both wheelsets of the bogie system. To the best of the knowledge of the author, none of the commercial wagon dynamics programs available in the market has the potential to predict what the RBD program has provided. Therefore the results of the RBD program (the output speed profile) in this section could not be validated using VAMPIRE.

The sequence of traction and braking torque applied to each wheelset is presented graphically in Fig. 5.24; a positive sign of torque represents traction and a negative sign represents braking. The initial speed of the bogie was set as 0.01 m/s to avoid numerical instability caused by floating point arithmetic in the calculation of the creepage (see Section 2.6).

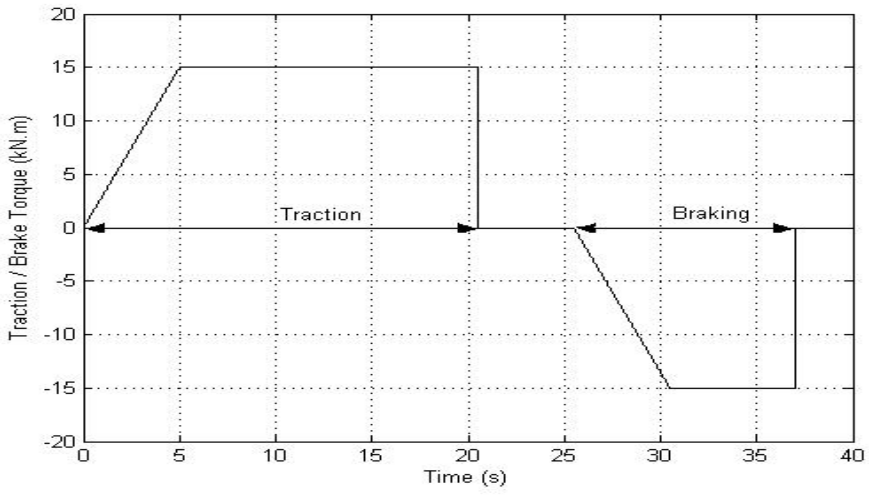

Figure 5.24. Traction/Braking torque profile

The traction torque was assumed to linearly increase from zero to 15 kN.m within 5 seconds, then remained constant until the bogie reached 20 m/s and then the traction torque was assumed to be released to zero. After maintaining a constant speed of 20 m/s for 5 seconds the brake torque was applied. Similar to traction torque, the brake torque was assumed to be gradually increased in 5 seconds from zero to 15 kN.m and was held at this value until the speed reduced to 10 m/s and then the brake was assumed to be released to zero.

The output acceleration and speed profile due to the traction/brake torque profile calculated by the RBD program is displayed in Fig. 5.25 and Fig.5.26 respectively. From t=0 sec to t=5 sec the longitudinal acceleration increased linearly from zero to a maximum value of 1.109 m/s^2 due to the gradual increment of the applied traction torque. During this time period the speed increment remained non-linear. After t=5 sec the acceleration was held constant until the bogie attained 20 m/s (approximately at t=20.5 sec). As the traction was reduced to zero, the acceleration reduced to zero between t=20.5 sec and t=25.5 sec. A similar trend was also observed during the braking process, where the speed reduction was not linear for the first five seconds of the braking process and then under the constant maximum braking torque the speed decreased linearly with a constant deceleration of about 1.109 m/s^2.

Fig.5.27 shows the output angular velocity of the leading and the trailing wheelsets and Fig 5.28 shows the total travel distance during the process which shows the bogie had travelled 496 m when the simulation ended. Fig.5.28 also reveals that the linear increment of travel distance happened at the constant speed section; i.e. between t=20.5 sec and t=25.5 sec and between t=37 and to t=40 sec.

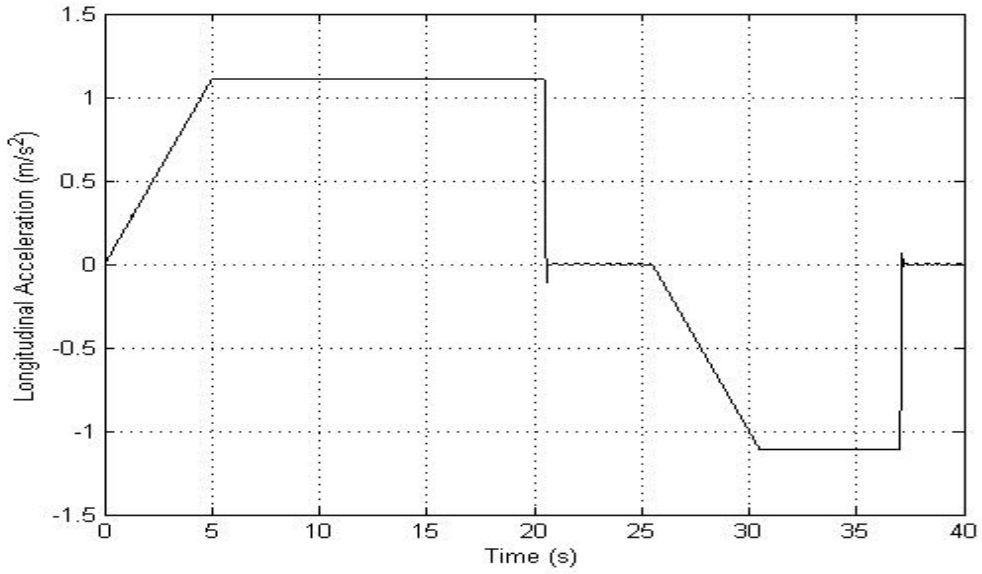

Figure 5.25. Output longitudinal acceleration

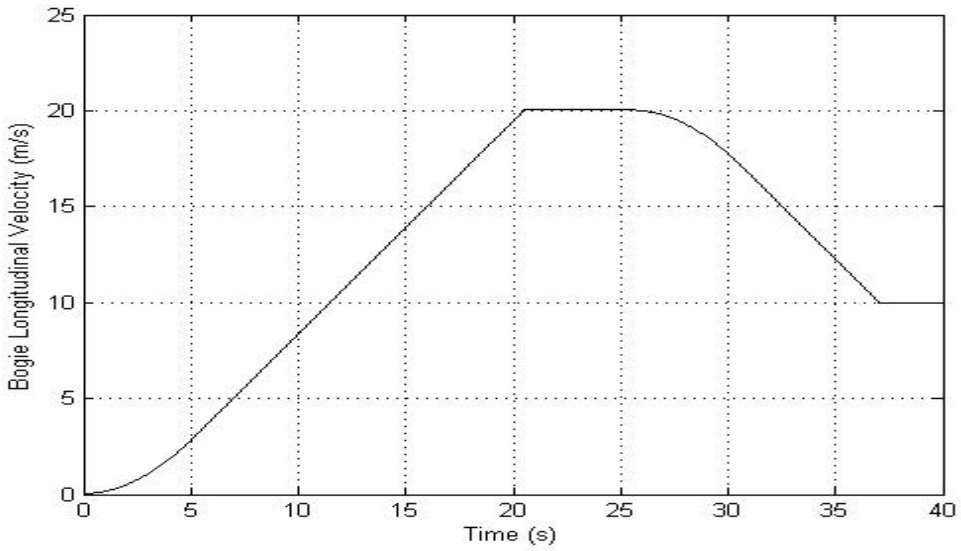

Figure 5.26. Output speed profile

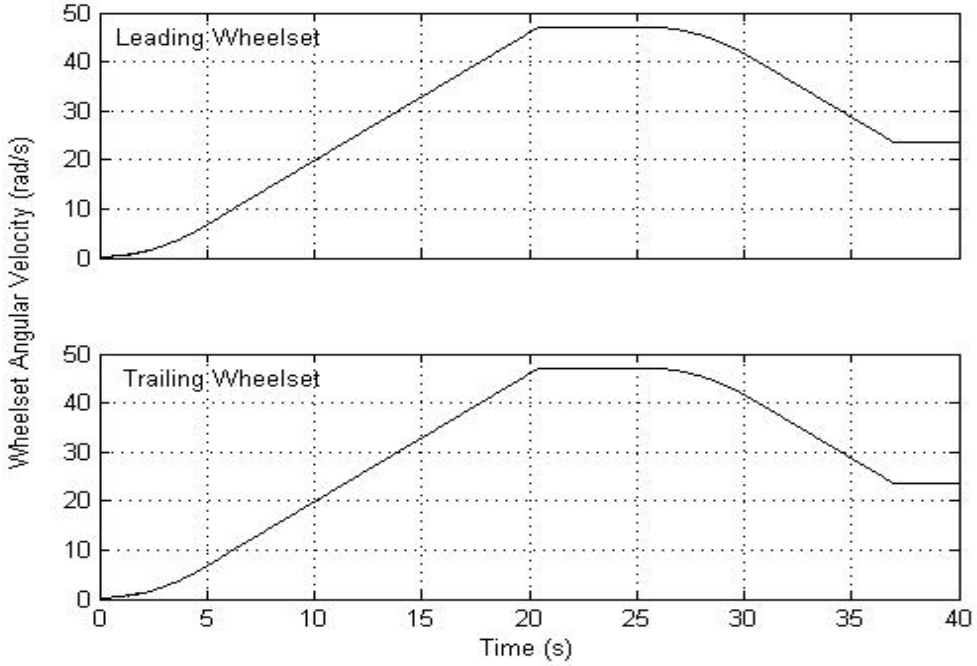

Figure 5.27. Output wheelset angular velocity (rad/s)

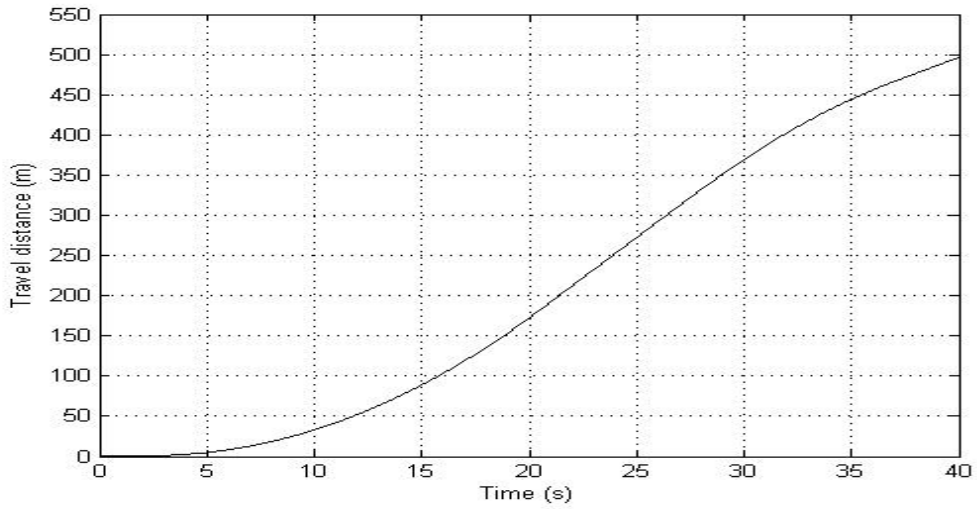

Figure 5.28. Travel distance

The speed profile and the wheelset angular velocity (as well as travel distance and wheelset rotation) calculated by the RBD program as the function of brake torque must be validated using an independent method. For this purpose, a full scale lab test was carried out. Chapter 6, 7 and 8 report this experiment and results including comparison with the simulation data set.

5.4.2. Bogie Pitch due to Longitudinal Force Application

As the longitudinal force due to traction or braking acts at a line below the centre of mass of the bogie frame, there exists a pitch moment acting on the bogie frame. Thus, during the application of the longitudinal force, pitch motion of the bogie frame is normally expected. Fig.5.29. shows the bogie frame pitch displacements during the application of the traction/braking profile of Fig.5.24. As expected, Fig.5.29 reveals that during traction, the pitch displacement attained negative values. The sudden reduction of the traction torque from 15 kN.m to zero (at t=20.5 sec) caused the bogie frame to experience a pitch oscillation when it ran at constant speed (between t=20.5 sec and t=25.5 sec). Then, during braking (t=25.5 sec and t=37 sec) the pitch displacement attained positive values. When the braking was suddenly released, the bogie frame experienced a pitch oscillation. These results show that the RBD program can truly model the longitudinal dynamics of the bogie due to application of traction and braking torques in a natural way.

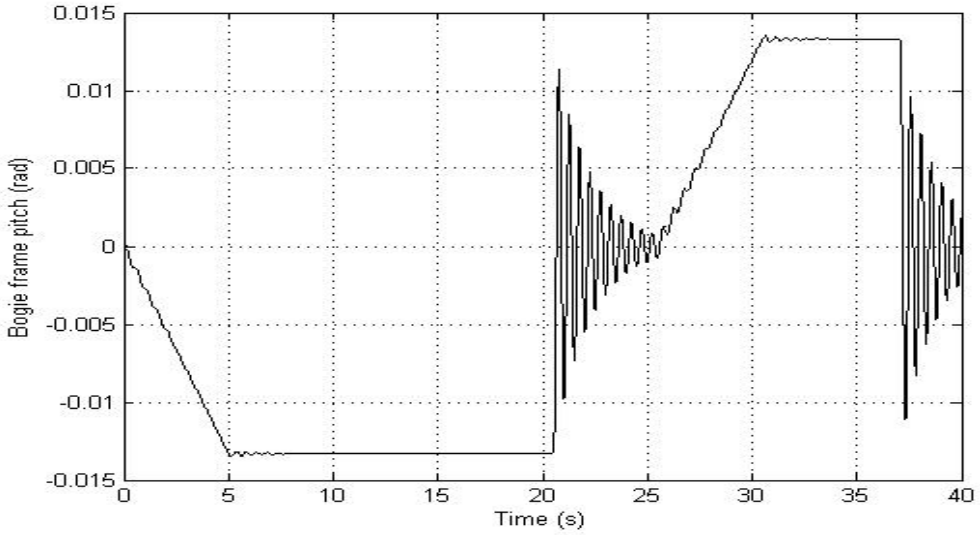

Figure 5.29. Bogie frame pitch calculated by RBD program

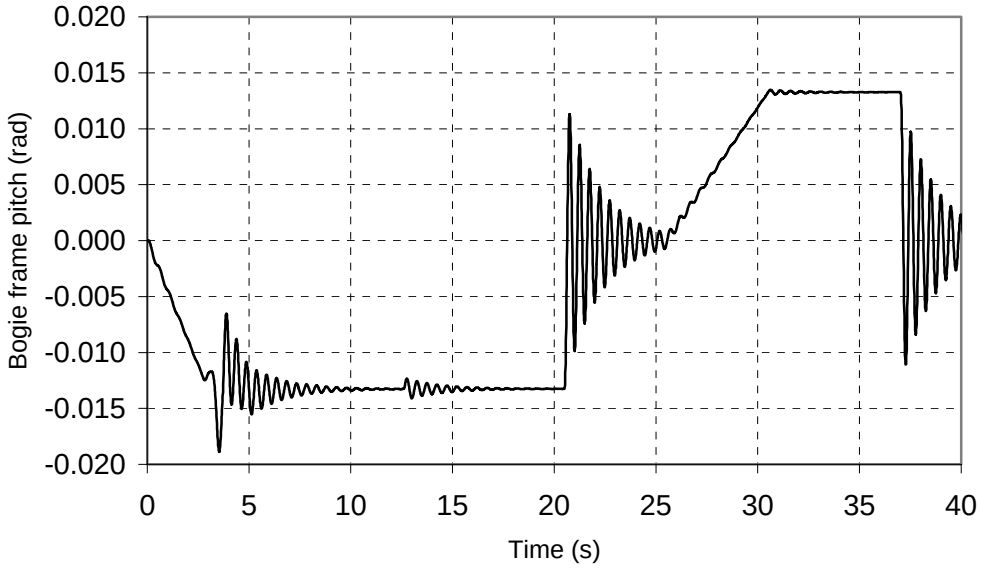

Figure 5.30. Bogie frame pitch calculated by VAMPIRE

The output speed profile in Fig.5.26 as well as the brake/traction torque profile of Fig.5.24 was then used as input for simulation in VAMPIRE. The bogie frame pitch displacement calculated by VAMPIRE is presented in Fig.5.30 which shows good

agreement with the prediction by the RBD program shown in Fig.5.29. Only small differences were found especially in the very low speed region (between 4 sec to 10 sec time period where the speed ranged between 3 m/s and 8 m/s). The pitch vibration predicted by VAMPIRE at low speed is not of practical significance and hence not further explored.

5.4.3. Bogie Lateral Dynamics under Variable Speed

The RBD program has the capability to calculate longitudinal dynamics due to traction and braking whilst calculating the response in the lateral and the vertical directions due to track irregularity. This section reports some examples of such simulation to investigate the lateral dynamics during traction and braking using the RBD program. The output speed profile calculated by the RBD program was then used as an input into VAMPIRE simulation and the results compared.

Lateral dynamics under traction

Two cases of traction application were investigated. First the traction torque was applied and increased gradually from zero to 15 kN.m in five seconds (normal application) as shown in Fig.5.31.(a) and then was held constant until the bogie attained 20 m/s (72 km/h). Fig.5.31.(b) shows the output speed profile (from the RBD program) due the input traction torque. While the bogie was under traction, the relevant section of the track was assumed to contain the sinusoidal lateral track irregularity as shown in Fig.5.32.

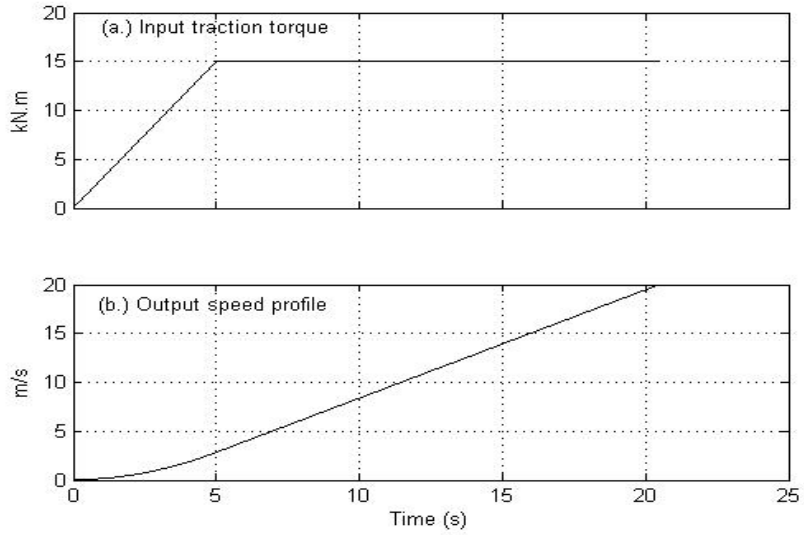

Figure 5.31. Input traction torque (normal application) and output speed profile calculated by RBD program

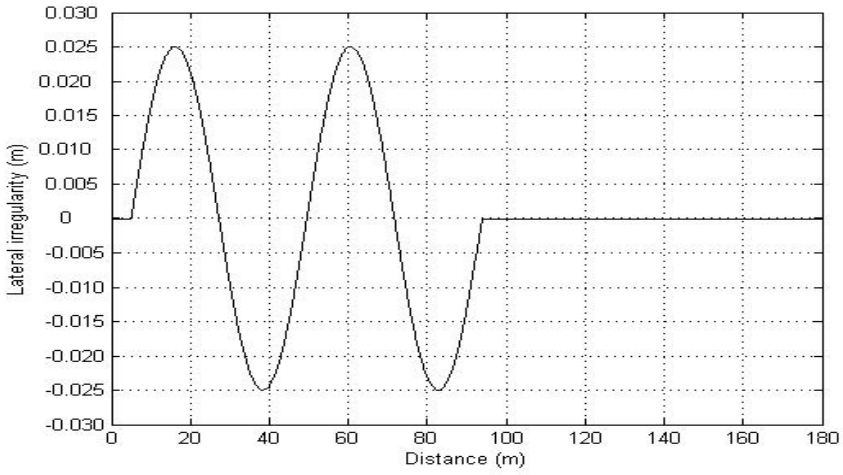

Figure 5.32. Input lateral track irregularity

Fig.5.33 shows the wheelset lateral displacement calculated by the RBD program during the traction application during movement over the track with irregularity. The figure reveals that the wheelsets experienced stable oscillation with maximum amplitude of approximately 9 mm. The frequency of oscillation increased with the

increase in speed as depicted by the shorter time period of the oscillation waves at the higher speed.

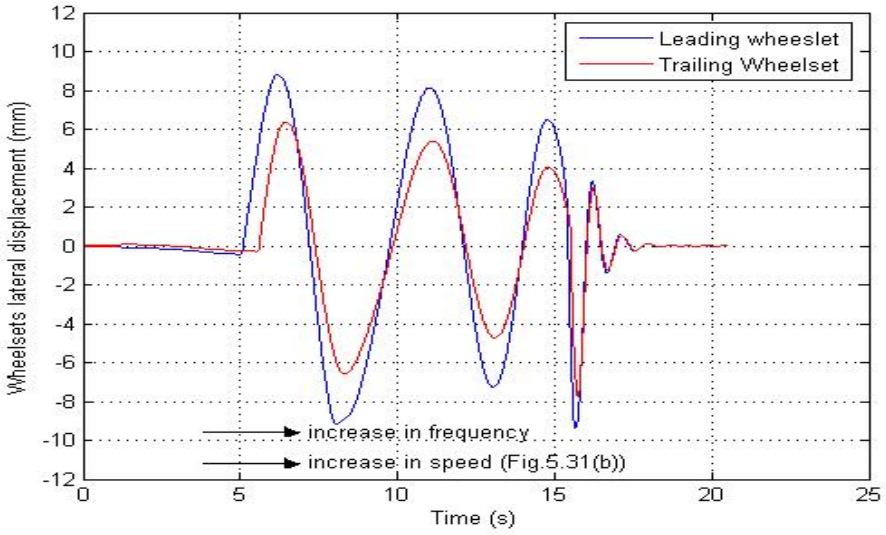

Figure 5.33. Wheelset lateral displacement during normal traction calculated by the RBD program

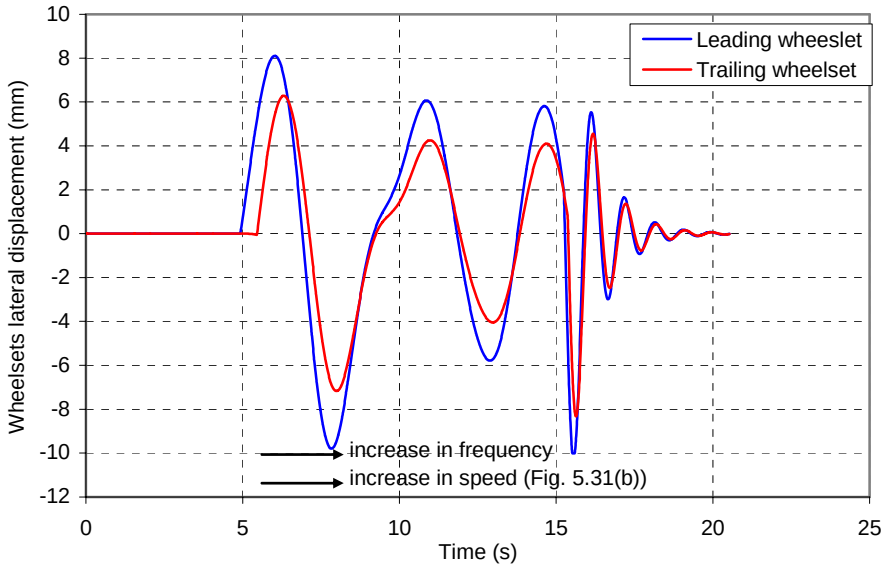

Figure 5.34. Wheelset lateral displacement during normal traction calculated by VAMPIRE

By inputting the traction torque as well as the speed profile calculated by the RBD program, an equivalent simulation was conducted by VAMPIRE. The wheelset lateral displacement calculated by VAMPIRE is exhibited in Fig.5.34. The result given by VAMPIRE agrees very well with the results of the RBD program shown in Fig.5.33. It should be remembered that VAMPIRE can calculate *only* if the speed profile was accurately input whereas the RBD program can determine the lateral dynamics in a natural way with the input of brake torque and track irregularity.

Quick application of traction torque was considered in the second case where the traction torque was increased from zero to 15 kN.m within one second before it was held constant until the bogie reached 20 m/s (72 km/h). The traction torque and the output speed profile are shown in Fig.5.35(a) and 5.35(b) respectively. As expected, compared to the normal traction application in Fig.5.31, the bogie attained the speed of 20 m/s quicker (in 18.2 seconds compared to 20.5 sec of normal traction).

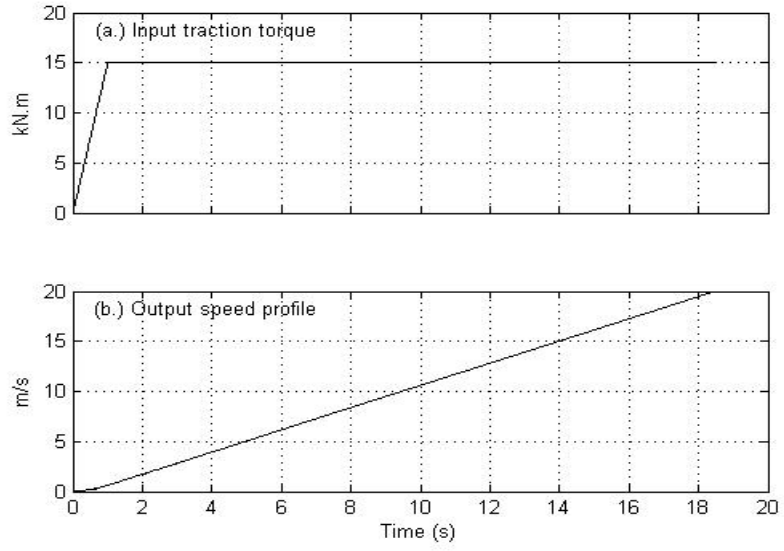

Figure 5.35. Input traction torque (quick application) and output speed profile calculated by RBD program

Lateral track irregularity shown in Fig 5.32 was also used in this second case. The lateral response of the bogie in the lateral direction calculated by the RBD program, in terms of wheelset lateral displacement, is shown in Fig.5.36. This result does not seem to be much different to the one just presented in Fig.5.33 from the simulation under normal application of traction. The wheelset oscillation remained stable with the frequency increased due to the increase in speed.

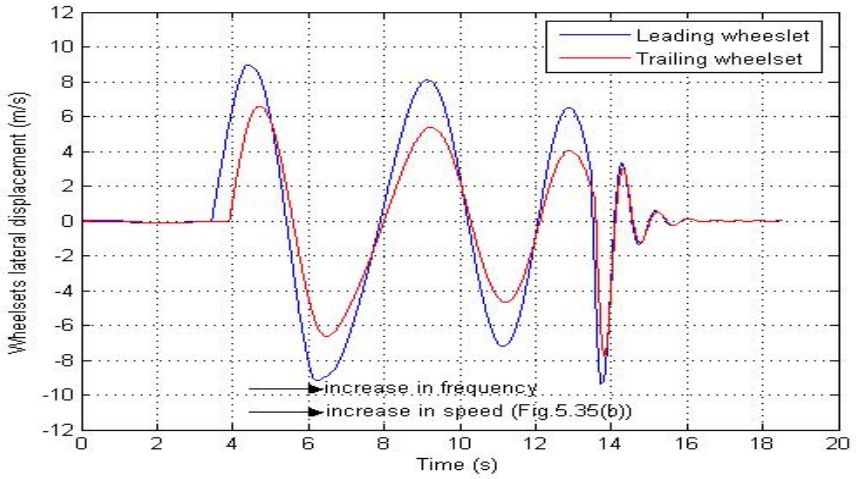

Figure 5.36. Wheelset lateral displacement during quick traction calculated - RBD program

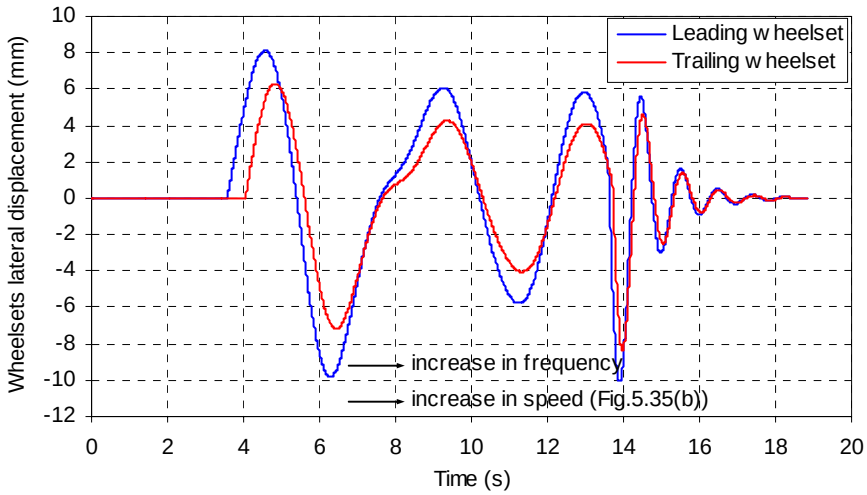

Figure 5.37. Wheelset lateral displacement during quick traction - VAMPIRE

The simulation using VAMPIRE also provided similar results as shown in Fig.5.37. These results show that as long as the speed of the bogie remains below its hunting speed level, its lateral response remains the same irrespective of the type of traction application (quick/normal).

Lateral dynamics under braking

Two cases of braking application were investigated. The simulation started at the constant speed 20 m/s (72 km/h). The braking was input as a negative pitch torque applied to the wheelset. First the normal application of braking torque was applied (brake torque increased gradually from zero to 15 kN.m in five seconds; from t=1 sec to t=6 sec) and then was held constant until the bogie stopped ("stop" here is assumed to be 0.01 m/s as absolute zero speed to avoid numerical instability) shown in Fig.5.38(a). Fig.5.38(b) shows the output speed profile. While braked, the bogie was running on the track that contained the sinusoidal lateral track irregularity as shown in Fig.5.32.

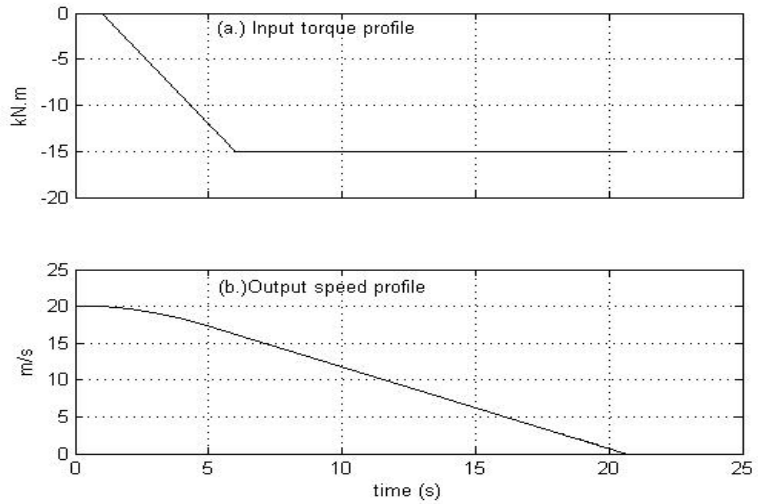

Figure 5.38. Input braking torque (normal application) and output speed profile

Fig.5.39 shows the wheelset lateral displacement during normal braking application during movement over the track with irregularity. This figure shows that the wheelsets

experienced stable oscillation with maximum amplitude of approximately 10.5 mm. The frequency of oscillation has decreased with the decrease in speed (shown by the longer time period of the oscillation waves at the higher speed). By inputting the braking torque as well as the speed profile calculated by the RBD program, an equivalent simulation was then conducted in VAMPIRE. The wheelset lateral displacement calculated by VAMPIRE is exhibited in Fig.5.40 which shows good agreement with that of the result calculated by the RBD program presented in Fig.5.39.

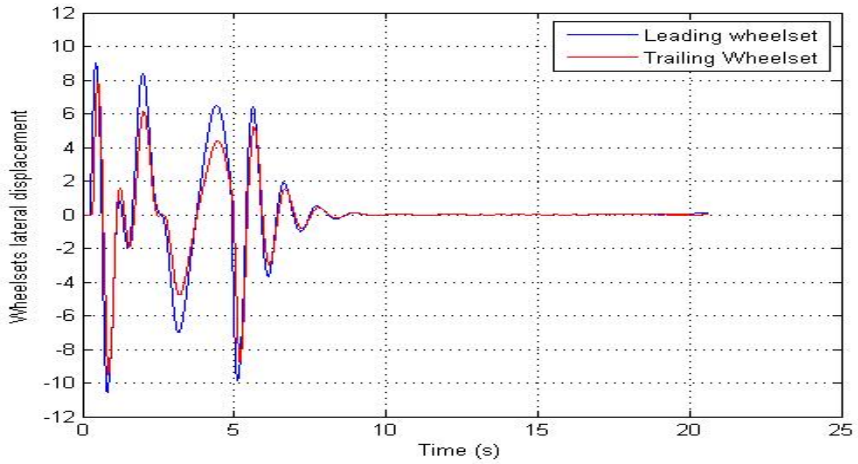

Figure 5.39. Wheelset lateral displacement during normal braking - RBD program

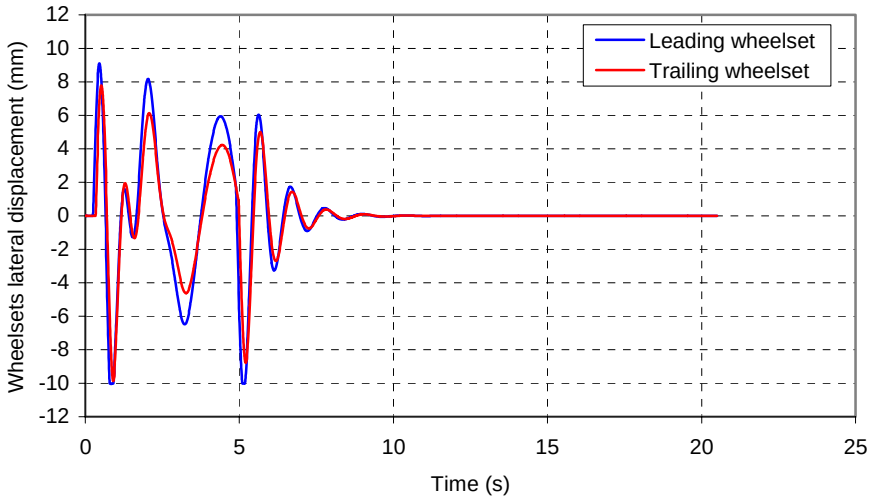

Figure 5.40. Wheelset lateral displacement during normal braking – VAMPIRE

The second case was concerned with quick braking application, where the braking torque was increased very quickly from zero to 15 kN.m within one second before it was held constant until the bogie stopped. As previously explained, “stop” here is assumed to be 0.01 m/s. The initial speed was 20 m/s (72 km/h). The braking torque and the output speed profiles are exhibited in Fig.5.41(a) and 5.41(b) respectively.

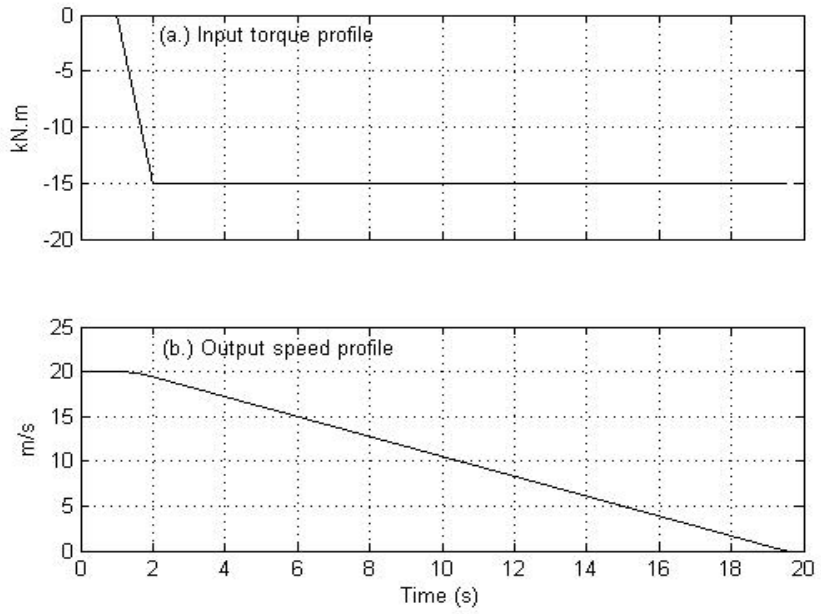

Figure 5.41. Input braking torque (quick application) and output speed profile

During the quick braking application the bogie was running on the same lateral track irregularity shown in Fig 5.32. The response of the bogie in the lateral direction calculated by the RBD program, which is represented by the wheelset lateral displacement, is shown in Fig.5.42. This result does not seem to be much different to the one presented in Fig.5.39 from the simulation under normal braking. The wheelset oscillation remained stable with the frequency decreased due to the decrease in speed. The simulation using VAMPIRE also provided similar result as shown in Fig.5.43.

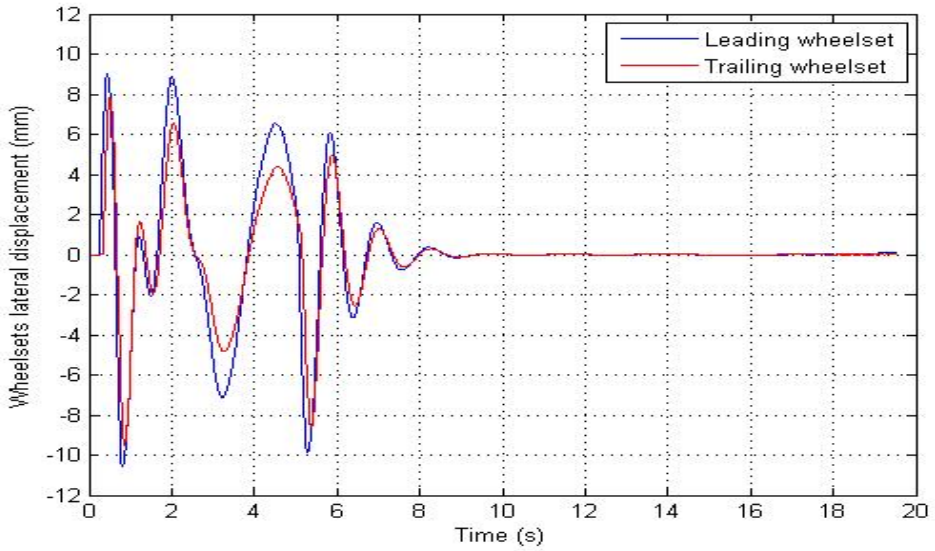

Figure 5.42. Wheelset lateral displacement under quick braking - RBD program

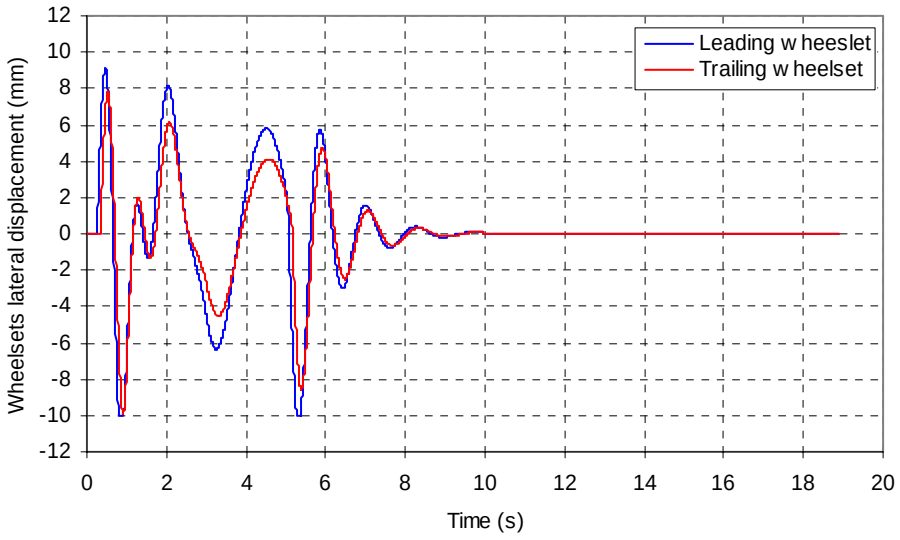

Figure 5.43. Wheelset lateral displacement under quick braking - VAMPIRE

5.5. BOGIE DYNAMICS UNDER HEAVY BRAKING

Two cases of heavy braking application were studied and reported in this section. Obviously these results containing wheel skid can not be compared with the simulations using VAMPIRE or other commercial package programs as they do not

explicitly include wheelset pitch in their formulation. The only option for validating these skid results is to carry out careful laboratory experiments capable of precisely measuring wheelset pitch and longitudinal position even under very low speed (due to restrictions in track lengths and increased levels of safety requirement). A full scale lab test satisfying all technical and safety needs was carried out for this purpose. Chapter 6, 7 and 8 report this experiment and results including comparison with the simulation data set.

Case #1 of heavy braking simulation deals with the application of a large brake torque to the leading wheelset while the trailing wheelset was left unbraked. The initial speed was set as V=25 m/s. Previous constant speed simulations (see Section 5.3) have shown that at this speed the bogie remained stable. At t=4 seconds a constant 60 kN.m brake torque was applied to the leading wheelset. The brake torque was specifically chosen large enough to initiate skidding.

The large brake torque application to the leading wheelset that exceeded the adhesion capacity between the wheel and the rail surface caused skidding of the leading wheelset as shown in Fig.5.44. Fig. 5.44(b) shows that the angular velocity of the leading wheelset has decreased rapidly to zero while the forward speed and the angular velocity of the trailing wheelset has remained much greater than zero (Fig.5.44 (a) and (c)).

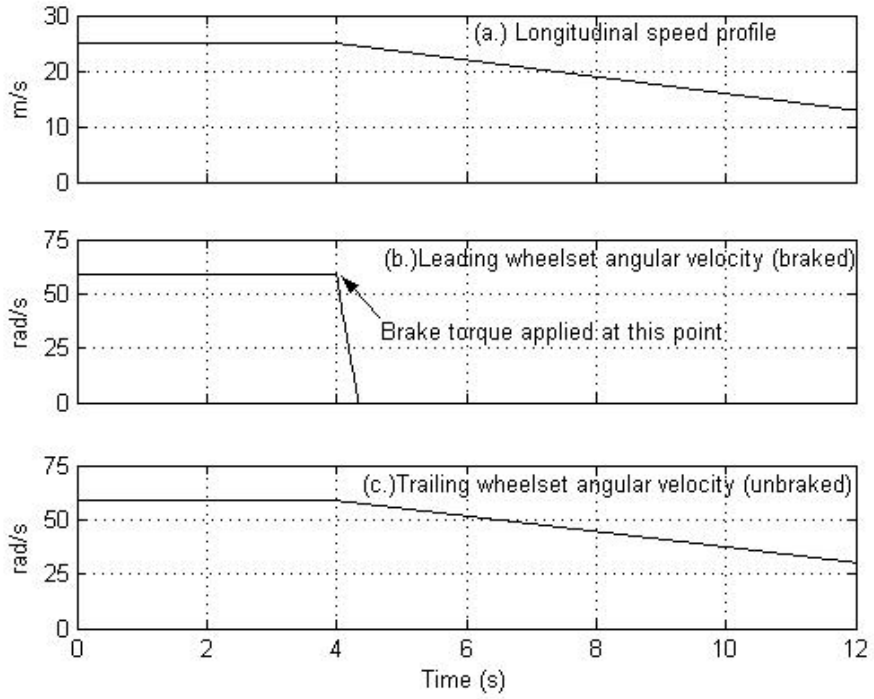

Figure 5.44. Skid on leading wheelset

Prior to the application of braking, the bogie was exposed to the sinusoid lateral irregularity of Fig 5.3. Fig.5.45 revealed that from just after passing this track section containing the lateral irregularity up until the application of brake (t=2 sec to t=4 sec) the bogie remained stable as shown by the reduction of lateral displacement. However it was found that after the application of the brake, which caused the wheelset to skid, the wheelset lateral oscillation became unstable exhibiting hunting motion. The amplitude of the lateral oscillation of the trailing wheelset which was left unbraked remained smaller than the oscillation of the braked leading wheelset.

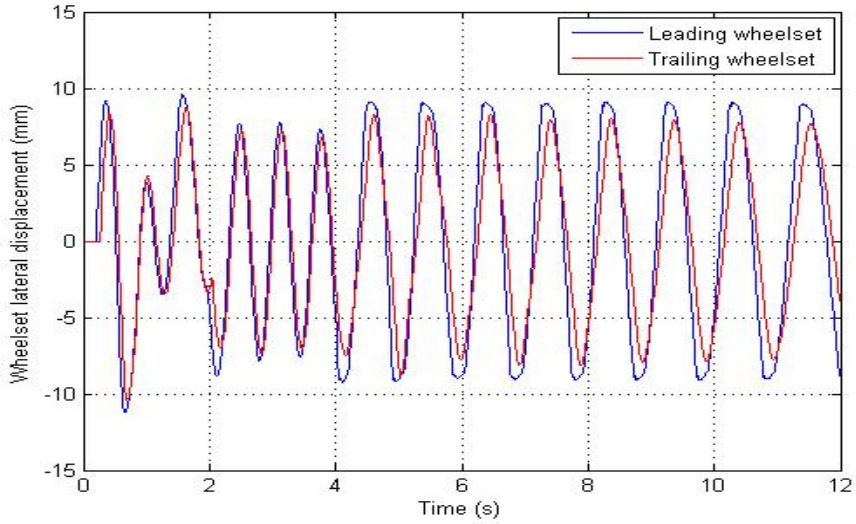

Figure 5.45. Lateral displacement; skid on leading wheelset

Case #2 of heavy braking was related to the application of 60 kN.m braking torques applied to both wheelsets. It caused skidding of both wheelsets as shown in Fig.5.46. This figure shows that the angular velocity of both wheelsets has rapidly decreased to zero while the speed remains non-zero. Prior to the application of braking, the bogie was exposed to the sinusoidal lateral irregularity to initiate the lateral oscillation. The lateral displacement time history is shown in Fig.5.47. Just after passing the track section that contains the lateral irregularity and up until the application of brake (t=2 sec to t=4 sec) the bogie has remained stable as shown by the reduction of lateral displacement. However after the application of the brake, which caused skidding on both wheelsets, the lateral movement of the wheelset became unstable with irregular form of oscillation. Even at low speed (less than 12 m/s), large oscillation wavelengths have been predicted.

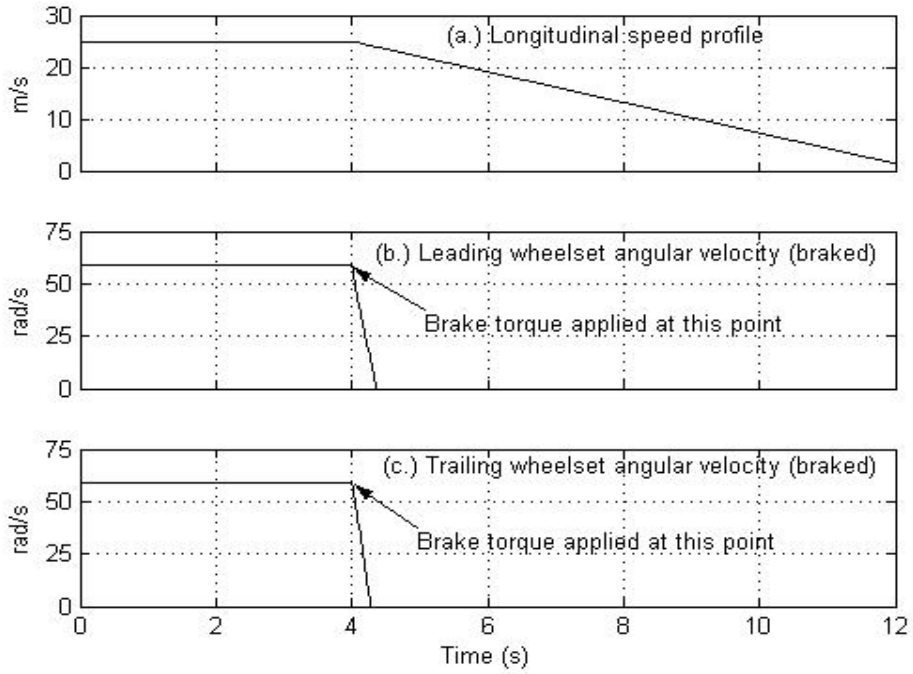

Figure 5.46. Skid on both wheelsets

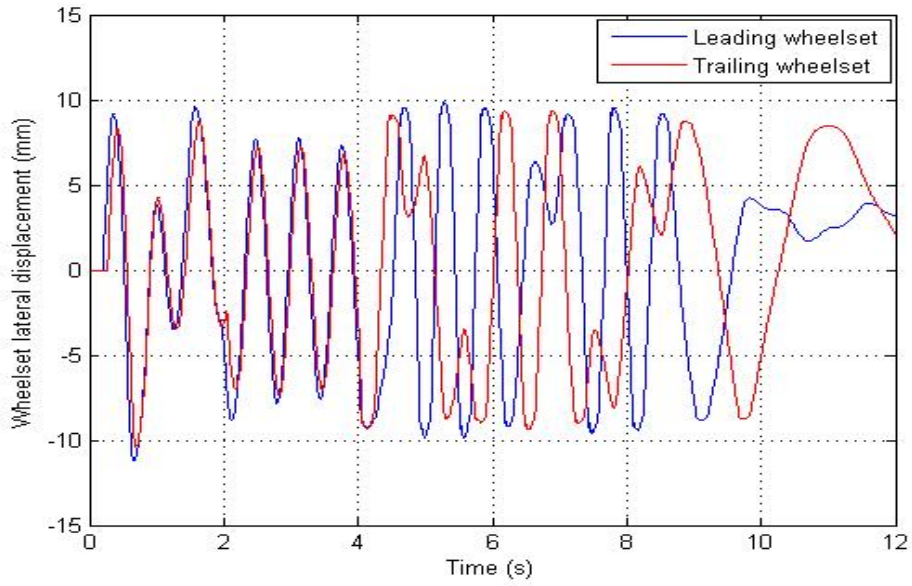

Figure 5.47. Lateral displacement, skid on both wheelsets

5.6. SUMMARY AND CONCLUSION

This chapter has described the capability of the RBD program in predicting the dynamics of the simplified two-axle bogies both under constant speed and under variable speed due to traction and brake. Novel features of the RBD program are the ability to evaluate the speed profile as a function of input braking / traction torques as well as explicitly determine wheelset angular velocity. These features have been demonstrated through examples in this chapter. The results have been validated whenever possible with the simulations using VAMPIRE that illustrated very good agreement. From the results we can draw the following conclusions:

- Under constant speed it was found that the bogie remained laterally stable up to 25 m/s. The insignificant difference between the results of RBD and VAMPIRE might have resulted from the different methods used in the calculation of the contact parameters and creep forces as well as the method of numerical integration used.

- The natural frequency of the bogie suspension in the vertical direction can be clearly detected by determining the frequency peaks which do not change with the change of the speed.

- The RBD program calculates the longitudinal dynamics of the bogie due to the application of traction and brake where the speed profile is an output of the simulation in a natural manner. The RBD program has the capability to effectively calculate the lateral and vertical dynamics simultaneously during the application of traction and braking.

- From the study of the lateral dynamics under variable speed it was found that, the lateral response of the bogie remains the same irrespective of the type of traction or braking application (quick/normal).

- The application of very large braking torques can lead to wheelset skid and tends to destabilize wheelset lateral oscillation. Simulation results showed that skidding on one wheelset or on both wheelsets of bogies affect the lateral oscillation differently.

- Part of the results of the RBD program, namely the speed profile and skid as a function of the application of brake torque, could only be validated using carefully designed experiments as other commercial dynamics packages do not explicitly account for these factors.